Electronic Structure and Molecular Conformation in the Excited Charge Transfer Singlet States of 9-Acridyl and Other Aryl Derivatives of Aromatic Amines

Jerzy Herbich* and Andrzej Kapturkiewicz*

Contribution from the Institute of Physical Chemistry, Polish Academy of Sciences, Kasprzaka 44/52, 01-224 Warsaw, Poland

Received July 21, 1997

Abstract: Donor (D)−acceptor (A) compounds containing aromatic amine as an electron donor and acridine as an acceptor show a low-energy CT absorption band which undergoes a red shift with increasing solvent polarity. Solvatochromic effects on the spectral position and profile of the stationary fluorescence spectra clearly indicate the CT character of the emitting singlet states of all the compounds studied. A band-shape analysis of the CT absorption and emission spectra leads to the quantities relevant for the electron transfer in the Marcus inverted region. The comparative determination of the electronic transition dipole moments corresponding to the $^1CT \leftarrow S_0$ absorption and the radiative charge recombination $^1CT \rightarrow S_0$ (M_{abs} and M_{flu}, respectively) made possible the estimation at the electronic coupling elements V_0 and V_1 between the ^1CT state and the ground state S_0 or the locally excited ^1LE state lying most closely in energy, respectively. To describe the properties of the excited ^1CT state of aryl derivatives of aromatic amines, the significant contributions of both of the above interactions together with the solvent induced changes of V_0 and V_1 have to be taken into account. In low polarity solvents the conformation of these compounds in the fluorescent $^1CT(f)$ state is more planar than that in the ground state (and in the unrelaxed Franck−Condon $^1CT(a)$ excited state), whereas in highly polar environment the compounds do not undergo any significant conformational changes accompanying the excited-state charge separation. The experimental and computational results led us to propose a simple model which allows one to predict the photophysical behavior of a particular D−A compound from the properties of its donor and acceptor moieties.

1. Introduction

Excited-state electron transfer is a fundamental reaction playing a crucial role in a variety of photophysical, photochemical, and biochemical processes (e.g., refs 1 and 2). The relatively simple systems in which the photoinduced intramolecular electron transfer (IET) can take place are donor (D)−acceptor (A) compounds formally linked by a single bond. The important issues related to the photophysics of these compounds are the electronic structure and conformation of the molecules in the excited charge transfer singlet states ^1CT. Information on the properties of these states can be obtained from the analysis of the charge transfer absorption $^1CT \leftarrow S_0$ and the radiative and radiationless charge recombination processes $^1CT \rightarrow S_0$. These reactions are described using a "Golden rule" type formula (as derived from a nonadiabatic theory of ET[3]) in which the rate is dependent on two quantities: (i) a Franck−Condon weighted density of states, which contains the dependence of the rate on the energetic and nuclear parameters such as the free energy gap ΔG_{CT}, the solvent (λ_s) and intramolecular (λ_i) reorganization energies, the intramolecular nuclear-electronic coupling, and the frequencies ν_i of the vibronic states coupled to ET (estimation of these parameters is possible from a band-shape analysis of the CT absorption[4,5] and/or fluorescence[5−13]) and (ii) the electronic matrix elements V_0 and V_i describing the electronic coupling between the lowest excited charge transfer state ^1CT and the ground state S_0 or the locally excited ^1LE states, respectively. The parameters V_0 and V_i can be obtained from the solvent polarity effects on the electronic transition dipole moments of the CT absorption (M_{abs}) and emission (M_{flu}).[7−11,13−22]

Two of the most intriguing aspects of the radiative charge recombination $^1CT \rightarrow S_0$ in large D−A π-systems such as

(1) *Photoinduced electron transfer (Parts A-D)*; Fox, M. A., Chanon, M., Eds.; Elsevier: Amsterdam, 1988.

(2) Kavarnos, G. J. *Fundamentals of Photoinduced Electron Transfer*; VCH: New York, 1994.

(3) E.g., (a) Ulstrup, J.; Jortner, J. *J. Chem. Phys.* **1975**, *63*, 4358. (b) Marcus, R. A.; Sutin, N. *Biochim. Biophys. Acta* **1985**, *811*, 265.

(4) (a) Hush, N. S. *Prog. Inorg. Chem.* **1967**, *8*, 391. (b) Hush, N. S. *Electrochim. Acta* **1968**, *13*, 1005. (c) Hush, N. S. *Coord. Chem. Rev.* **1985**, *64*, 135.

(5) Marcus, R. A. *J. Phys. Chem.* **1989**, *93*, 3078 and references cited therein.

(6) Gould, I. R.; Farid, S. *J. Photochem. Photobiol. A: Chem.* **1992**, *65*, 133.

(7) Gould, I.R.; Young, R. H.; Moody, R. E.; Farid, S. *J. Phys. Chem.* **1991**, *95*, 2068.

(8) Gould, I. R.; Noukakis, D.; Gomez-Jahn, L.; Young, R. H.; Goodman, J. L.; Farid, S. *Chem. Phys.* **1993**, *176*, 439.

(9) Gould, I. R.; Noukakis, D.; Gomez-Jahn, L.; Goodman, J. L.; Farid, S. *J. Am. Chem. Soc.* **1993**, *115*, 4405.

(10) Gould, I. R.; Young, R. H.; Mueller, L. J.; Farid, S. *J. Am. Chem. Soc.* **1994**, *116*, 8176.

(11) Gould, I. R.; Young, R. H.; Mueller, L. J.; Albrecht, A. C.; Farid, S. *J. Am. Chem. Soc.* **1994**, *116*, 8188.

(12) Cortes, J.; Heitele, H.; Jortner, J. *J. Phys. Chem.* **1994**, *98*, 2527 and references cited therein.

(13) Kapturkiewicz, A.; Herbich, J.; Karpiuk, J.; Nowacki, J. *J. Phys. Chem. A* **1997**, *101*, 2332.

S0002-7863(97)02474-8 CCC: $15.00
Published on Web 01/27/1998

biaryls,[23,24] aryl derivatives of aromatic amines,[25−29] various compounds related to biphenyl,[30,31] and *N*-carbazoyl derivatives of aromatic nitriles[13,32] concern its mechanism and the high probability of this process. The electronic transition dipole moments M_{abs} and M_{flu} have been analyzed[7−10,13−15] employing the Mulliken two-state model,[16,17] i.e., the electronic coupling between the ^{1}CT and S_0 states. On the other hand, to account for the solvent dependence of the CT fluorescence of 4-(9-anthryl)-*N*,*N*-dimethylaniline (ADMA) and its derivatives[18] or the large intensity of the CT absorption bands in rigidly bridged D−B−A molecules[14,19] a three-state mixing model has been applied. This model includes, in addition to the S_0 and ^{1}CT states, a low lying ^{1}LE state of the appropriate symmetry (this intensity "borrowing" mechanism has been advanced by Murrell[33] and Mulliken and Person[34]). The mixing of charge transfer and locally excited states has been previously treated several times, e.g., the importance of the latter mechanism in exciplexes has been presented by Beens and Weller[35] and Van der Auweraer et al.[36] Recently,[11,20−22] the significant solvent polarity effects on M_{flu} have been quantitatively described in terms of the interaction between the ^{1}CT and ^{1}LE states.

Another challenging problem concerns the structure of the D−A molecules in the fluorescent ^{1}CT state. Contrary to the twisted intramolecular charge transfer (TICT) state model,[26] it has been concluded[13,28b,31] that the excited-state conformation of the D^+ and A^- moieties in large conjugate π-systems is far from perpendicular. 9-Anthryl derivatives of *N*,*N*-dimethylanilines[28b] and 9,9′-bianthryl[23b] are most probably flattened upon excitation; the conformation of the nitrile derivatives of 3,6-di-*tert*-butylcarbazole in the lowest ^{1}CT state seems to be similar to that in the ground state.[13] These hypotheses are based on the calculations of the ground-state structure, the estimation of the intramolecular reorganization energies from the bandshape analysis of the stationary CT emission (and absorption) spectra, and the solvent and temperature effects on the electronic transition dipole moments M_{flu}. Very recently,[22] the quantitative analysis of the CT absorption and emission spectra of 4-(9-anthryl)julolidine (AJ) and 4-(9-acridyl)julolidine (BJ) has shown that the electronic and molecular structure of these compounds in the solvent-equilibrated fluorescent ^{1}CT(f) states depend on the environment. In low polarity solvents the conformation of the compounds in the ^{1}CT(f) states is more planar than that in the ground state (and in the Franck−Condon excited state ^{1}CT(a) reached upon absorption), whereas in highly polar media these compounds do not undergo any significant conformational changes accompanying the excited-state charge separation. These effects are most probably generated by the strength of the coupling between the ^{1}CT and ^{1}LE states, which depends on the respective energy gap. The solvent-dependent electronic structure of 9-anthryl derivatives of *N*,*N*-dimethylanilines in the lowest ^{1}CT state has been previously deduced from the transient absorption studies by Okada et al.[37]

This work is a part of our study of the photophysics[13,22,28,31,38] and electrochemiluminescence[39−43] of the relatively large aromatic D−A compounds formally linked by a single bond.

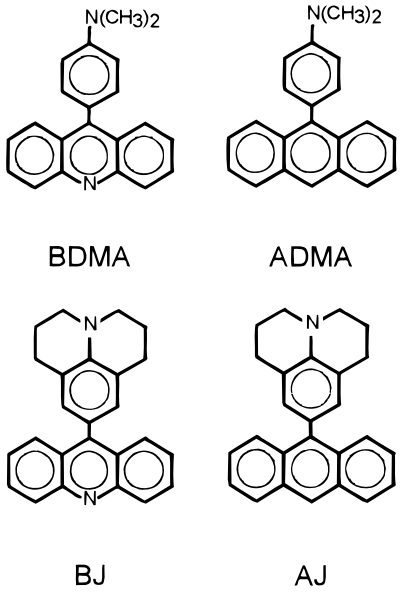

Figure 1. Formulas of *p*-anthryl and *p*-acridyl derivatives of *N*,*N*-dimethylaniline (ADMA and BDMA, respectively) and julolidine (AJ and BJ, correspondingly).

(14) (a) Oevering, H. Ph.D. Dissertation, University of Amsterdam, Amsterdam, the Netherlands, 1988. (b) Oevering, H.; Verhoeven, J. W.; Paddon-Row, M. N.; Warman, M. J. *Tetrahedron* **1989**, *45*, 4751.
(15) Oliver, A. M.; Paddon-Row, M. N.; Kroon, J.; Verhoeven, J. W. *Chem. Phys. Lett.* **1992**, *191*, 371.
(16) Mulliken, R. S. *J. Am. Chem. Soc.* **1952**, *74*, 811.
(17) Beratan, D.; Hopfield, J. J. *J. Am. Chem. Soc.* **1984**, *106*, 1584.
(18) (a) Mataga, N.; Murata, Y. *J. Am. Chem. Soc.* **1969**, *91*, 3144. (b) Mataga, N. In *The Exciplex*; Gordon, M., Ware, W. R., Eds.; Academic: New York, 1975. (c) Masaki, S.; Okada, T.; Mataga, N.; Sakata, Y.; Misumi, S. *Bull. Chem. Soc. Jpn.* **1976**, *49*, 1277.
(19) (a) Pasman, P. Ph.D. Dissertation, University of Amsterdam, Amsterdam, the Netherlands, 1980. (b) Pasman, P.; Rob, F.; Verhoeven, J. W. *J. Am. Chem. Soc.* **1982**, *104*, 5127.
(20) Bixon, M.; Jortner, J.; Verhoeven, J. W. *J. Am. Chem. Soc.* **1994**, *116*, 7349 and references cited therein.
(21) Verhoeven, J. W.; Scherer, T.; Wegewijs, B.; Hermant, R. M.; Jortner, J.; Bixon, M.; Depaemelaere, S.; De Schryver, F. C. *Recl. Trav. Chim. Pays-Bas* **1995**, *114*, 443.
(22) Herbich, J.; Kapturkiewicz, A. *Chem. Phys. Lett.* **1997**, *273*, 8.
(23) (a) Rettig, W.; Zander, M. *Ber. Bunsen-Ges. Phys. Chem.* **1983**, *87*, 143. (b) Mataga, N.; Nishikawa, S.; Okada, T. *Chem. Phys. Lett.* **1996**, *257*, 327.
(24) Dobkowski, J.; Grabowski, Z. R.; Paeplow B.; Rettig, W.; Koch, K. H.; Müllen, K.; Lapouyade, R. *New J. Chem.* **1994**, *18*, 525 and references cited therein.
(25) (a) Okada, T.; Fujita, T.; Kubota, M.; Masaki, S.; Mataga, N.; Ide, R.; Sakata, Y.; Misumi, S. *Chem. Phys. Lett.* **1972**, *14*, 563. (b) Okada, T.; Fujita, T.; Mataga, N. *Z. Physik. Chem. NF* **1976**, *101*, 57.
(26) (a) Grabowski, Z. R.; Rotkiewicz, K.; Siemiarczuk, A.; Cowley, D. J.; Baumann, W. *Nouv. J. Chim.* **1979**, *3*, 443. (b) Siemiarczuk, A.; Grabowski, Z. R.; Krówczyński, A.; Asher, M.; Ottolenghi, M. *Chem. Phys. Lett.* **1977**, *51*, 315. (c) Siemiarczuk, A.; Koput, J.; Pohorille, A. *Z. Naturforsch.* **1982**, *37a*, 598.
(27) Tominaga, K.; Walker, G. C.; Jarzęba, W.; Barbara, P. F. *J. Phys. Chem.* **1991**, *95*, 10475.
(28) (a) Herbich, J.; Kapturkiewicz, A. *Chem. Phys.* **1991**, *158*, 143. (b) Herbich, J.; Kapturkiewicz, A. *Chem. Phys.* **1993**, *170*, 221.
(29) Onkelinx, A.; De Schryver, F. C.; Viaene, L.; Van der Auweraer, M.; Iwai, K.; Yamamoto, M.; Ichikawa, M.; Masuhara, H.; Maus, M.; Rettig, W. *J. Am. Chem. Soc.* **1996**, *118*, 2892.
(30) Van Damme, W.; Hofkens, J.; De Schryver, F. C.; Ryan, T. G.; Rettig, W.; Klock, A. *Tetrahedron* **1989**, *45*, 4693.
(31) Herbich, J.; Waluk, J. *Chem. Phys.* **1994**, *188*, 247.
(32) Rettig, W.; Zander, M. *Chem. Phys. Lett.* **1982**, *87*, 229.
(33) Murrell, J. N. *J. Am. Chem. Soc.* **1959**, *81*, 5037.
(34) Mulliken, R. S.; Person, W. B. In *Molecular Complexes: A Lecture and Reprint Volume*; Wiley: New York, 1969.
(35) Beens, H.; Weller, A. In *Organic Molecular Photophysics*; Birks, J. B., Ed.; Wiley: New York, 1975; p 159.
(36) Van der Auweraer, M.; Swinnen, A. M.; De Schryver, F. C. *J. Chem. Phys.* **1982**, *77*, 4110.
(37) Okada, T.; Mataga, N.; Baumann, W.; Siemiarczuk, A. *J. Phys. Chem.* **1987**, *91*, 4490.
(38) Herbich, J.; Kapturkiewicz, A.; Nowacki, J. *Chem. Phys. Lett.* **1996**, *262*, 633.
(39) Kapturkiewicz, A.; Grabowski, Z. R.; Jasny, J. *J. Electroanal. Chem.* **1990**, *279*, 55.
(40) (a) Kapturkiewicz, A. *J. Electroanal. Chem.* **1991**, *302*, 131. (b) Kapturkiewicz, A. *Z. Physik. Chem.* **1991**, *170*, 87.
(41) Kapturkiewicz, A. *Chem. Phys.* **1992**, *166*, 259.
(42) Kapturkiewicz, A. *J. Electroanal. Chem.* **1993**, *348*, 283.
(43) Kapturkiewicz, A.; Herbich, J.; Nowacki, J. *Chem. Phys. Lett.* **1997**, *275*, 355.

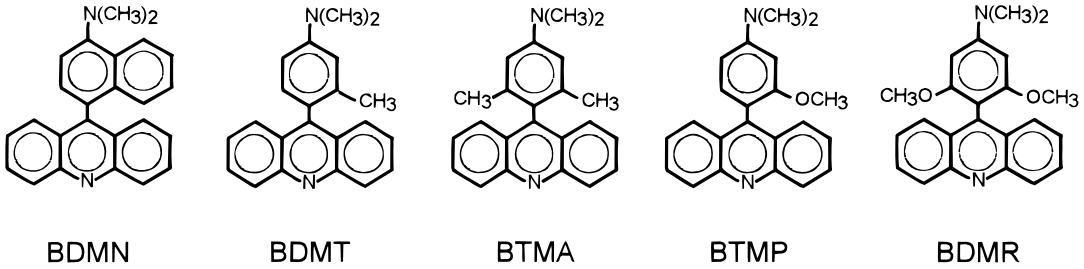

Figure 2. Formulas of *p*-acridyl derivatives of aromatic amines and their abbreviations used in the text.

In order to understand the mechanism of the radiative (^{1}CT $\leftarrow$ S_0 and ^{1}CT $\rightarrow$ S_0) and nonradiative charge transfer transitions and to determine the changes of the molecular structure related to the excited-state electron transfer, in this paper we address the problems of the electronic structure and molecular conformation of three series of D−A compounds. (i) 9-Anthryl and 9-acridyl derivatives of *N*,*N*-dimethylaniline, DMA {ADMA and 4-(9-acridyl)-*N*,*N*-dimethylaniline (BDMA), respectively}, and julolidine (AJ and BJ, correspondingly): The detailed investigations of these compounds[22,28] (Figure 1) showed very similar photophysical properties of the related pairs of D−A compounds containing anthryl or acridyl as an electron acceptor; the differences in thermodynamics and kinetics of the photoinduced electron transfer seem to be induced mainly by the larger electron affinity of the acridyl subunit than that of the anthryl moiety. This finding together with the relatively low ionization potential of julolidine with respect to that of DMA result in the corresponding lowering of the energy of the ^{1}CT states which provides the well separated red-shifted CT absorption band in BJ[22] and BDMA.[44] This fact made possible to estimate independently, from the CT absorption and fluorescence investigations, the electronic coupling elements V_0 and V_1 between the lowest excited charge transfer state ^{1}CT and the ground state S_0 or the locally excited ^{1}LE state lying most closely in energy, respectively. (ii) BJ and BDMA (Figure 1), 4-(9-acridyl)-*N*,*N*-dimethyl-1-naphthylamine (BDMN), 4-(9-acridyl)-3,*N*,*N*-trimethylaniline (BDMT), 4-(9-acridyl)-3,5,*N*,*N*-tetramethylaniline (BTMA), 4-(9-acridyl)-3-methoxy-*N*,*N*-dimethylaniline (BTMP), and 4-(9-acridyl)-3,5-dimethoxy-*N*,*N*-dimethylaniline, BDMR (Figure 2): These D−A acridine derivatives have been selected mainly because of their different ground-state conformation (the acceptor and donor are close to perpendicularity in BDMN or less twisted in BJ and BDMA). (iii) Aryl derivatives of DMA, 4-(1-naphthyl)-*N*,*N*-dimethylaniline (NDMA), 4-(1-pyrenyl)-*N*,*N*-dimethylaniline (PDMA), 4-(3-fluoranthyl)-*N*,*N*-dimethylaniline (FDMA),[28] and 4-(9-phenanthryl)-*N*,*N*-dimethylaniline (HDMA).[29] Formulas of these compounds are shown in Figure 3.

In this work we describe a detailed study of the solvent effects on the spectral position and profile of the CT absorption and fluorescence spectra as well as on the oscillator strength of the CT absorption, CT emission quantum yields, and excited-state depopulation kinetics of the two former series of compounds. The factors that control the excited-state electron transfer are determined by varying the donor and the acceptor subunits as well as the solvent polarity. Our comparative investigations show a possibility to predict the photophysical behavior of a particular D−A compound from the properties of its donor and acceptor subunits. The latter group of compounds is selected to test the hypothesis.

(44) Baumann, W.; Raber, W. Unpublished results.

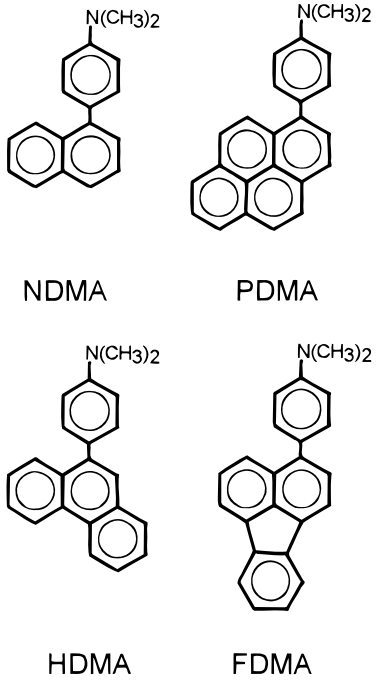

Figure 3. Formulas of aryl derivatives of *N*,*N*-dimethylaniline and their abbreviations used in the text.

2. Experimental Section

2.1. Materials. 4-(9-Acridyl)-*N*,*N*-dimethyl-1-naphthylamine, 4-(9-acridyl)julolidine, 4-(9-acridyl)-*N*,*N*-dimethylaniline and its derivatives, 4-(9-acridyl)-3,*N*,*N*-trimethylaniline, 4-(9-acridyl)-3,5,*N*,*N*-tetramethylaniline, 4-(9-acridyl)-3-methoxy-*N*,*N*-dimethylaniline, and 4-(9-acridyl)-3,5-dimethoxy-*N*,*N*-dimethylaniline have been synthesized similarly to the procedure described in ref 45. The crude compounds were purified by recrystallization from propanol-2.

The solvents used for absorption and emission studies are as follows: methylcyclohexane (MCH), butyl ether (BE), isopropyl ether (IPE), ethyl ether (EE), butyl acetate (BA), ethyl acetate (EA), tetrahydrofuran (THF), 1,2-dichloromethane (DCM), 1,2-dichloroethane (DCE), *N*,*N*-dimethylformamide (DMF), acetonitrile (ACN), and dimethyl sulfoxide (DMSO). These solvents were of spectroscopic or fluorescence grade (Aldrich and Merck). Butyronitrile, BN (Merck, for synthesis), was purified as previously described.[13] All solvents did not show any traces of luminescence and have been selected to cover the wide range of the static dielectric permittivity values ϵ.[46]

2.2. Instrumentation and Procedures. Absorption spectra were recorded using a Shimadzu UV 3100 spectrometer. Fluorescence and excitation spectra were measured by means of the Jasny spectrofluorimeter[47] and were corrected for the spectral sensitivity of the instrument. For the quantum yield determinations, the solutions had identical optical densities at the excitation wavelength and were

(45) Ullmann, F.; Bader, W.; Labhardt, H. *Ber. Deut. Chem. Ges.* **1907**, *40*, 4795.

(46) Reichardt, C. *Solvent Effects in Organic Chemistry*; Verlag: New York, 1979.

(47) Jasny, J. *J. Lumin.* **1978**, *17*, 143.

deaerated by the saturation with preliminary purified and dried argon to avoid fluorescence quenching by oxygen. Quinine sulfate in 0.1 N H_2SO_4 ($\Phi_f = 0.51$),[48a] rhodamine 101 in ethanol ($\Phi_f = 0.98 \pm 0.02$),[48bc] and ruthenium(II) trisbipyridyl complex $Ru(bpy)_3Cl_2$ in water ($\Phi_f = 0.062$)[48d] served as the quantum yield standards. Sulfuric acid and ethanol were of fluorescence grade (Merck). Water was used after four distillations over $KMnO_4$ in a quartz apparatus.

Fluorescence lifetimes were obtained using the sampling method (with MSG 350 S nitrogen laser with pulse duration of 0.6 ns (fwhm) as the excitation source and boxcar BCl 280 on the detection side).[49] The experimental decay curves were analyzed by the single-curve method using the DECAN deconvolution program (kindly obtained from Prof. F. C. De Schryver, Catholic University of Leuven, Belgium) with the reference convolution based on the Marquardt algorithm;[50] the χ^2 test and the distribution of residuals served as the main criteria in the evaluation of fit quality. In all of the cases studied the fluorescence decay was monoexponential on the nanosecond scale of observation.

Semiempirical quantum chemical calculations have been performed using the AM1 method (from HYPERCHEM package developed by Hypercube Inc.). Other calculations (e.g., band-shape analysis of the CT fluorescence) were made by means of the least-squares method using a Sigma Plot package from Jandel Corp.

3. Results and Discussion

3.1. Absorption and Fluorescence. Room temperature low-energy absorption bands and fluorescence spectra of BDMR and BTMP, BDMN, BTMA, BDMT, BDMA, and BJ are presented in Figures 4−6. Absorption and emission data are collected in Tables 1 and 2, respectively. The comparison of the absorption spectra with that of acridine[51−53] clearly indicates a presence of the bands corresponding to the following transitions: (i) $^1CT \leftarrow S_0$ (which appears at the red-energy side of the absorption spectrum) and (ii) two $^1(\pi,\pi^*) \leftarrow S_0$ localized in the acceptor subunit (which are assigned to the final ^1L_a and ^1L_b excited states in Platt's notation; for acridine the 0,0 transition of the relatively intense short-axis polarized $^1L_a \leftarrow S_0$ band lies about 26 000 cm^{-1} and its spectral position is about 1000−2000 cm^{-1} below a very weak $^1L_b \leftarrow S_0$ transition[51]). Whereas these transitions are superimposed in the first absorption band of BDMN, a prominent long-wave shoulder attributed to the $^1CT \leftarrow S_0$ transition is observed for BTMA, BDMT, BDMR, and BTMP. A well separated CT absorption band appears for BJ and BDMA. The latter finding is generated by (i) the relatively low ionization potential of julolidine (which decreases the CT states energy in BJ with respect to the other members of the series containing acridyl as an electron acceptor) and/or (ii) the more planar conformation of the two latter compounds (which increases the probability of the radiative transitions, see Tables 1 and 4) than that of the other molecules in the series. The CT absorption band of BJ and BDMA shows a clear red shift with increasing solvent polarity (Figure 7).

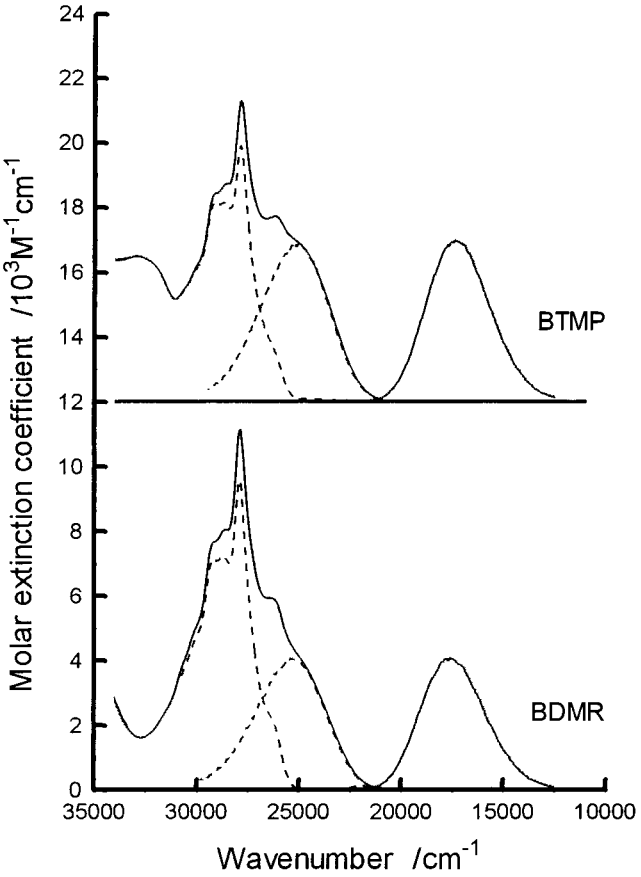

Figure 4. Room temperature absorption ($\epsilon(\tilde{\nu})$ vs $\tilde{\nu}$) and corrected fluorescence ($I(\tilde{\nu}_f)$ vs $\tilde{\nu}_f$) spectra of 4-(9-acridyl)-3,5-dimethoxy-*N*,*N*-dimethylaniline (BDMR) and 4-(9-acridyl)-3-methoxy-*N*,*N*-dimethylaniline (BTMP) in tetrahydrofuran. Spectra of BTMP are shifted along the *y*-axis by a factor of 1.2×10^4. Solid lines—low energy absorption bands (left part) and CT fluorescence spectra (right part). Dashed lines: (i) the lowest CT absorption band obtained under the assumption that the reduced CT absorption (as plotted in the form $\epsilon(\tilde{\nu})/\tilde{\nu}$ vs $\tilde{\nu}$) and CT emission spectra (i.e., a plot of the normalized reduced intensity $I(\tilde{\nu}_f)/\tilde{\nu}_f^3$ vs $\tilde{\nu}_f$) exhibit a mirror relationship with respect to the crossing point; (ii) absorption band corresponding to $^1(\pi,\pi^*) \leftarrow S_0$ excitations localized in the acridyl moiety (being dominated by the $^1L_a \leftarrow S_0$ transition). The latter band is a result of a subtraction of the lowest CT absorption band from the total absorption spectrum (matching of the computed and experimental low energy parts of the absorption served as the main criterion of the quality of the separation procedure).

According to the theory of dielectric polarization,[54] this behavior of the absorption band is expected for the transitions from a state with a small dipole moment to a state with a larger one (eq 1). Assuming a point dipole situated in the center of the spherical cavity and neglecting the mean solute polarizability α in the states involved in the transition ($\alpha \cong \alpha_e \cong \alpha_g \cong 0$), the solvatochromic effects on the spectral position of the CT absorption spectra can be given by[55−57]

$$hc\tilde{\nu}_{abs}^{CT} \cong hc\tilde{\nu}_{abs}^{vac} - \frac{2\vec{\mu}_g(\vec{\mu}_e - \vec{\mu}_g)}{a_o^3}\left[\frac{\epsilon - 1}{2\epsilon + 1} - \frac{1}{2}\frac{n^2 - 1}{2n^2 + 1}\right] \quad (1)$$

where $hc\tilde{\nu}_{abs}^{CT}$ and $hc\tilde{\nu}_{abs}^{vac}$ are the energies related to the spectral

(48) (a) Velapoldi, R. A. National Bureau of Standards 378, Proc. Conf. NBS, Gaithersburg, ms 1972; p 231. (b) Kubin, R. F.; Fletcher, A. N. *J. Lumin.* **1982**, *27*, 455. (c) Karstens, T.; Kobs, K. *J. Phys. Chem.* **1980**, *84*, 1871. (d) Cook, M. J.; Lewis, A. P.; McAuliffe, G. S. G.; Skarda, V.; Thomson, A. J. *J. Chem. Soc., Perkin Trans II.* **1984**, 1293.

(49) Karpiuk, J.; Grabowski, Z. R. *Chem. Phys. Lett.* **1989**, *160*, 451.

(50) Marquardt, D. W. *J. Soc. Ind. Appl. Math.* **1963**, *11*, 431.

(51) Steiner, R. P.; Michl, J. *J. Am. Chem. Soc.* **1978**, *100*, 6861.

(52) (a) Zanker, V.; Schmid, W. *Chem. Ber.* **1957**, *90*, 2253. (b) Zanker, V.; Schiefele, G. *Z. Elektrochem.* **1958**, *62*, 86. (c) Zanker, V.; Schmid, W. *Chem. Ber.* **1959**, *92*, 615. (d) Perkampus, H.-H.; Kortüm, K. *Z. Physik. Chem. NF*, **1967**, *56*, 73. (e) Seiffert W.; Limbach, H.; Zanker, V.; Mantsch, H. H. *Tetrahedron* **1970**, *26*, 2663. (f) Inoue, H.; Hoshi, T.; Masamoto, T.; Shiraishi, J.; Tanizaki, Y. *Ber. Bunsen-Ges. Phys. Chem.* **1971**, *75*, 441.

(53) Wagner, R. W.; Hochmann, P.; Al-Bayoumi, M. A. *J. Mol. Spectr.* **1975**, *54*, 167.

(54) Böttcher, C. J. F. In *Theory of Electric Polarization*; Van Belle, O. C., Bordewijk, P., Rip, A., Eds.; Elsevier: Amsterdam, 1973; Vol. 1.

(55) Onsager, L. *J. Am. Chem. Soc.* **1936**, *58*, 1486.

(56) (a) Lippert, E. *Z. Naturforsch.* **1955**, *10a*, 541. (b) Mataga, N.; Kaifu, Y.; Koizumi, M. *Bull. Chem. Soc. Jpn.* **1955**, *28*, 690.

(57) Liptay, W. In *Excited States*; Lim, E. C., Ed.: Academic Press: New York, 1974; p 129.

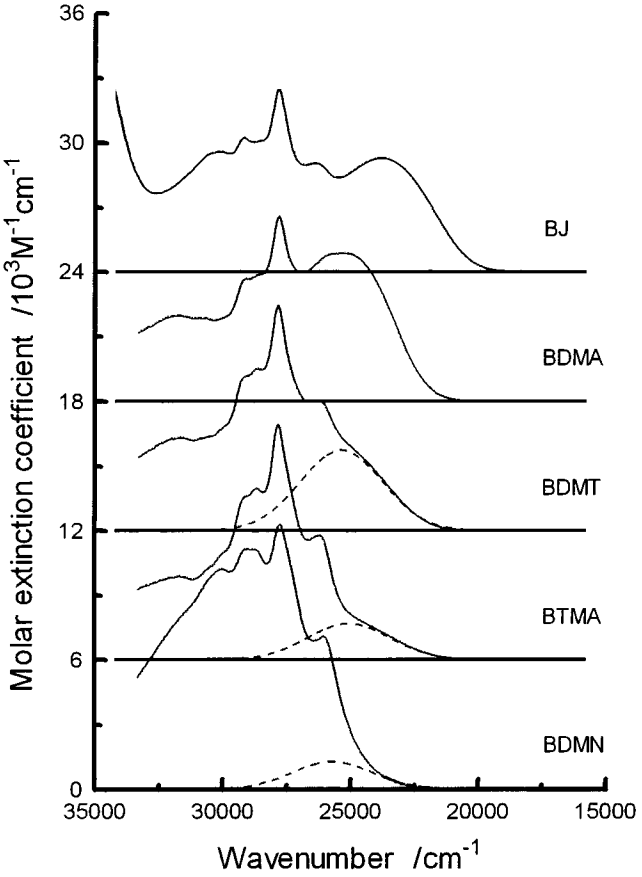

Figure 5. Room temperature absorption spectra recorded in tetrahydrofuran for 4-(9-acridyl)-*N*,*N*-dimethyl-1-naphthylamine (BDMN), *p*-acridyl derivatives of various *N*,*N*-dimethylanilines {4-(9-acridyl)-3,5,*N*,*N*-tetramethylaniline (BTMA), 4-(9-acridyl)-3,*N*,*N*-trimethylaniline (BDMT), and 4-(9-acridyl)-*N*,*N*-dimethylaniline (BDMA)}, and 4-(9-acridyl)julolidine (BJ). Spectra of BTMA, BDMT, BDMA, and BJ are shifted along the *y*-axis by a factor of 6×10^3. Dashed lines—spectral position and shape of the low-energy CT absorption band obtained according to the procedure described in the text and in the caption to Figure 4.

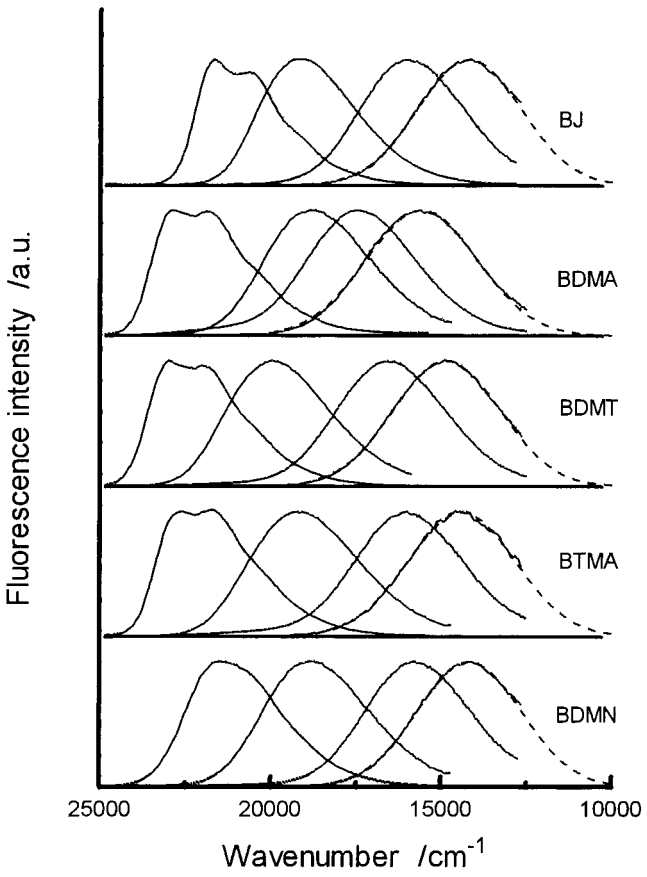

Figure 6. Corrected and normalized room temperature CT fluorescence spectra of BDMN, BTMA, BDMT, BDMA, and BJ in methylcyclohexane, butyl ether, tetrahydrofuran, and butyronitrile (from left to right, respectively). Dashed lines correspond to the numerical fits using eqs 14a and 14b.

positions of the CT absorption maxima in solutions and to the value extrapolated to the gas-phase, respectively; $\vec{\mu}_g$ and $\vec{\mu}_e$ are the dipole moments of the solute in the ground and excited state, correspondingly; a_o is the effective radius of the Onsager's cavity,[55] ϵ is the static dielectric constant, and n is the refractive index of the solvent.

9-Acridyl derivatives of aromatic amines, similarly as other aryl derivatives of aromatic amines[25−29] and N-bonded derivatives of carbazole containing various aromatic nitriles as electron acceptors,[13,32] emit a single fluorescence band at room temperature (Figure 6). A considerable red shift of their spectral position (Table 2, Figures 6−8) and the increase of the Stokes shift and of the emission bandwidth with increasing solvent polarity point to the CT character of the fluorescent states.

3.2. Excited-State Dipole Moments. The results collected in Table 2 show that the lifetimes of the fluorescent ^{1}CT states of the D−A acridine derivatives are in a nanosecond range, i.e., these states live about two or three orders of magnitude longer than the solvent orientational relaxation times.[27,58] Due to this fact, the excited-state dipole moments $\vec{\mu}_e$ can be estimated by the fluorescence solvatochromic shift method. Under the same assumptions as used for eq 1, Lippert[56a] and Mataga[56b] have obtained the following expression

$$hc\tilde{\nu}_{flu}^{CT} \cong hc\tilde{\nu}_{flu}^{vac} - \frac{2\vec{\mu}_e(\vec{\mu}_e-\vec{\mu}_g)}{a_o^3}\left[\frac{\epsilon-1}{2\epsilon+1} - \frac{1}{2}\frac{n^2-1}{2n^2+1}\right] \quad (2a)$$

where $\tilde{\nu}_{flu}^{CT}$ and $\tilde{\nu}_{flu}^{vac}$ are the spectral positions of the solvent-equilibrated CT fluorescence maxima and the value extrapolated to the gas-phase, respectively.

In polar media the D−A compounds containing acridyl as an electron acceptor show a satisfying linear correlation (Figures 7 and 8) between the energy $hc\tilde{\nu}_{flu}^{CT}$ and the solvent polarity function $\{f(\epsilon) - 0.5\ f(n)\}$, where

$$f(\epsilon) = \frac{\epsilon-1}{2\epsilon+1}; \quad f(n) = \frac{n^2-1}{2n^2+1} \quad (2b)$$

The expressions 1 and 2 relate the measured quantities to the excited-state dipole moments $\vec{\mu}_e$. The fluorescence experiments in polar solvents allow us to determine directly the values of $\vec{\mu}_e(\vec{\mu}_e - \vec{\mu}_g)/a_o^3$ (Table 3) and $\tilde{\nu}_{flu}^{vac}$ (eq 2a). The values of the excited state dipole moments μ_e, estimated with the effective radius of the spherical Onsager cavity $a_o \approx 0.65$ nm (as evaluated from the molecular dimensions of the compounds calculated by AM1 and molecular mechanics[59] methods) are about 30 D. On the other hand, (i) eq 1 can be used to determine

(58) (a) Grampp, G.; Jaenicke, W. *Ber. Bunsen-Ges. Phys. Chem.* **1991**, *95*, 904. (b) Fawcett, W.R.; Opatto, M. *Angew. Chem., Int. Ed. Engl.* **1994**, *33*, 2131.

(59) (a) Allinger, N. L. *Adv. Phys. Org. Chem.* **1976**, *13*, 1. (b) Ground-state geometry optimizations were done by molecular mechanics (MMX force field, PCMODEL from Serena Software).

Table 1. Room Temperature Absorption Data for 9-Acridyl Derivatives of Aromatic Amines in Tetrahydrofuran[d]

compd	$\tilde{\nu}_{abs}^{CT}$,[a] cm^{-1}	$\epsilon(\tilde{\nu}_{abs}^{CT})$[b]	$\epsilon(\tilde{\nu})_{LE}$,[b] M^{-1} cm^{-1}	$\epsilon(\tilde{\nu})_{LE}/\epsilon(\tilde{\nu})_{ref}$	M_{abs}, D
BJ	23 800	5300	8500	0.68	2.5
BDMA	25 200	6800	6950	0.55	2.7
BTMP	~25 250	~4900	~7900	~0.63	~2.3
BDMT	~25 350	~3850	~9300	~0.74	~2.0
BDMR	~25 400	~4100	~9550	~0.76	~2.1
BTMA	~25 050	~1650	~10 550	~0.84	~1.4
BDMN[c]	≈25 700	≈1200	≈12 000	≈0.95	≈1

[a] Scatter of results: ±50 cm^{-1} for BJ and BDMA, and about ±150 cm^{-1} for other compounds. [b] Error is about 5−10%. [c] Results for BDMN are only roughly estimated. [d] $\epsilon(\tilde{\nu}_{abs}^{CT})$, $\epsilon(\tilde{\nu})_{LE}$, and $\epsilon(\tilde{\nu})_{ref}$ denote the molar absorption coefficients either at the spectral position of the maximum of the CT absorption band ($\tilde{\nu}_{abs}^{CT}$) or at the most intense vibronic band of the $^1L_a \leftarrow S_0$ transition in the D−A compound (LE) or in acridine (ref), respectively. M_{abs} is the transition dipole moment corresponding to the $^1CT \leftarrow S_0$ absorption (see text).

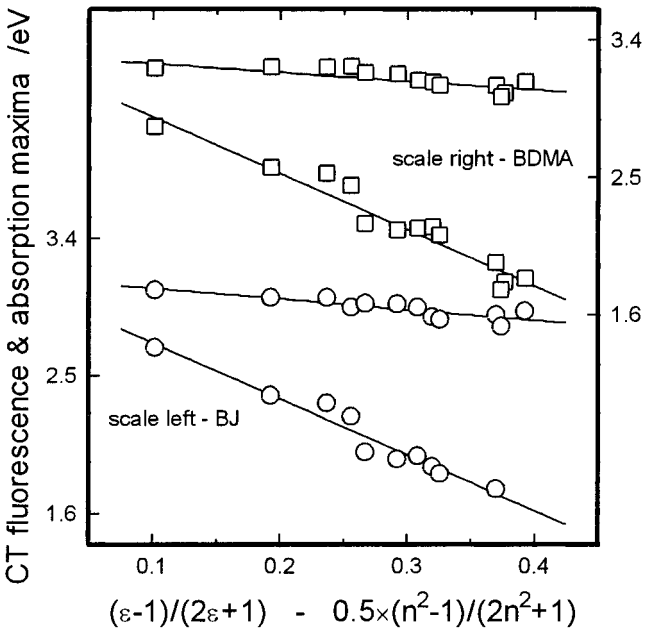

Figure 7. Solvatochromic shift of the energy related to the CT absorption (upper signs) and fluorescence maxima (lower signs) for BJ (circles) and BDMA (squares) as a function of solvent polarity (eq 2b) corresponding to the model formulated by Lippert[56a] and Mataga[56b] (eqs 1 and 2, respectively). Correlations take into account the whole range of the solvents (see text).

the values of $\vec{\mu}_g(\vec{\mu}_e - \vec{\mu}_g)/a_o^3$ and $\tilde{\nu}_{abs}^{vac}$ in the case of the well separated CT absorption bands and (ii) under the assumption that the CT fluorescence corresponds to the state reached directly upon excitation, the quantity $(\vec{\mu}_e - \vec{\mu}_g)^2/a_o^3$ can be evaluated from the solvation effects on the Stokes shift[56a,57]

$$hc(\tilde{\nu}_{abs}^{CT} - \tilde{\nu}_{flu}^{CT}) = hc(\tilde{\nu}_{abs}^{vac} - \tilde{\nu}_{flu}^{vac}) + \frac{2(\vec{\mu}_e - \vec{\mu}_g)^2}{a_o^3}\left[\frac{\epsilon - 1}{2\epsilon + 1} - \frac{n^2 - 1}{2n^2 + 1}\right] \quad (3)$$

The corresponding values of $(\vec{\mu}_e - \vec{\mu}_g)^2/a_o^3$ could be estimated for the compounds showing a distinctly separated CT absorption band, i.e., BJ[22] and BDMA. Moreover, the comparative observation of the solvent dependence of the CT absorption and fluorescence band positions for the two latter compounds made possible to estimate the ratio of μ_e to the ground-state dipole moment μ_g. The results presented in Figure 7 lead to the value $(\mu_e/\mu_g) \approx 5.8$. With $\mu_g = 4.5(\pm 0.4)$ D (this value has been determined for BDMA by means of the electrooptical absorption and emission measurements[44]) we obtain $\mu_e \approx 26$ D. The large value of $\mu_e - \mu_g \approx 21.5$ D ($\vec{\mu}_g$ and $\vec{\mu}_e$ are parallel due to the symmetry of BJ and BDMA) corresponds to a charge separation of about 0.45 nm, which roughly agrees with the center-to-center distance between the donor and acceptor moieties of the compounds.

In a low polarity environment, however, similarly as it has been observed for ADMA and related compounds,[25,60,61] and other aryl derivatives of aromatic amines,[28a] a deviation from the linear correlation between the energy $hc\tilde{\nu}_{flu}^{CT}$ and the solvent polarity function proposed by Lippert and Mataga[56] is observed (Figure 8). To explain this effect, Baumann et al.[60] have postulated a considerable contribution of the induced dipole moment (as reflecting the solvent-induced changes of the electronic distribution in a solute). In fact, the fit can be improved by taking into account the solute polarizability effects, e.g., according to the model formulated by McRae[62] (Figure 8, cf. also ref 28a). Under similar assumptions as used for eqs 1 and 2, except $\alpha_e/a_o^3 = \alpha_g/a_o^3 = 0.5$, it follows that[57,62]

$$hc\tilde{\nu}_{abs}^{CT} \cong hc\tilde{\nu}_{abs}^{vac} - \frac{2\vec{\mu}_g(\vec{\mu}_e - \vec{\mu}_g)}{a_o^3}\left[\frac{\epsilon - 1}{\epsilon + 2} - \frac{1}{2}\frac{n^2 - 1}{n^2 + 2}\right] \quad (4a)$$

$$hc\tilde{\nu}_{flu}^{CT} \cong hc\tilde{\nu}_{flu}^{vac} - \frac{2\vec{\mu}_e(\vec{\mu}_e - \vec{\mu}_g)}{a_o^3}\left[\frac{\epsilon - 1}{\epsilon + 2} - \frac{1}{2}\frac{n^2 - 1}{n^2 + 2}\right] \quad (4b)$$

with the solvent polarity function $\{F(\epsilon) - 0.5\ F(n)\}$, where

$$F(\epsilon) = \frac{\epsilon - 1}{\epsilon + 2}; \quad F(n) = \frac{n^2 - 1}{n^2 + 2} \quad (4c)$$

It should be pointed out, however, that a more probable explanation of the nonlinear relationship between the spectral positions of the CT fluorescence maxima $\tilde{\nu}_{flu}^{CT}$ of aryl derivatives of aromatic amines and the Lippert−Mataga solvent polarity function (eq 2b) concerns the dependence of the electronic structure of the fluorescent states on solvation (as it has been proposed by Mataga[25b]). This hypothesis is in agreement with the finding that the effect increases with the energy of the excited ^1CT states—the deviation is considerably smaller for BJ or AJ than that for the other D−A acridine or anthracene derivatives, respectively (the polarizability effects for these compounds are expected to be similar). Due to a relatively small energy gap between the lowest ^1CT state and the locally excited ^1LE states in a nonpolar medium one can expect a significant contribution of the $^1(\pi,\pi^*)$ character to the wave function $^1\Psi_{CT}$ of the fluorescent $^1CT(f)$ state

(60) (a) Baumann, W; Petzke, F.; Loosen, K.-D. *Z. Naturforsch.* **1979**, *34a*, 1070. (b) Baumann, W. *Z. Naturforsch.* **1981**, *36a*, 868. (c) Detzer, N.; Baumann, W.; Schwager, B.; Fröhling, J.-C.; Brittinger, C. *Z. Naturforsch.* **1987**, *42a*, 395.

(61) Herbich, J.; Dobkowski, J.; Rullière, C.; Nowacki, J. *J. Lumin.* **1989**, *44*, 87.

(62) McRae, E. G. *J. Phys. Chem.* **1957**, *61*, 562.

Table 2. Solvent Effects on the Spectral Position of the CT Fluorescence Maxima ($\tilde{\nu}_{flu}^{CT}$), Quantum Yields (Φ_f), Decay Times (τ) and Resulting Radiationless (k_{nr}) and Radiative (k_f) Rate Constants, and Electronic Transition Dipole Moments (M_{flu}) of 9-Acridyl Derivatives of Aromatic Amines at Room Temperature

compd	solvent	$\tilde{\nu}_{flu}^{CT}$,[a] cm^{-1}	Φ_f[b]	τ,[b] ns	k_{nr}, $\times 10^7$ s^{-1}	k_f, $\times 10^7$ s^{-1}	M_{flu}, D
BJ	MCH	21 675	0.33	3.0	22.3	11.0	3.5
	BE	19 150	0.37	7.7	8.2	4.8	2.8
	THF	15 950	0.24	12.4	6.1	1.9	2.3
	BN	14 200	0.014	1.7	58.0	0.85	1.9
BDMA	MCH	22 800, 21 900	0.06	0.5	18.8	12.0	3.4
	BE	20 650	0.27	3.7	19.7	7.3	3.1
	THF	17 450	0.50	15.3	3.3	3.3	2.7
	BN	15 650	0.16	8.1	10.4	2.0	2.5
BTMP	MCH	21 700	0.47	3.7	14.3	12.7	3.7
	BE	20 450					
	THF	17 250					
	BN	15 400	0.41	17.7	3.4	2.3	1.7
BDMT	MCH	22 850, 22 000	0.43	4.7	12.1	9.1	3.0
	BE	19 950	0.30	9.4	7.4	3.2	2.2
	THF	16 550	0.23	18.0	4.3	1.3	1.8
	BN	14 850	0.051	6.5	15.3	0.77	1.7
BDMR	MCH	21 150	0.53	8.5	5.5	6.2	2.7
	BE	20 450					
	THF	17 250					
	BN	15 475	0.074	9.0	10.3	0.82	1.6
BTMA	MCH	22 625, 21 775	0.12	3.2	27.5	3.8	2.0
	BE	19 175	0.14	9.9	8.7	1.4	1.5
	THF	16 000	0.11	16.7	5.3	0.66	1.4
	BN	14 400	0.023	5.3	18.4	0.43	1.3
BDMN	MCH	21 300	0.305	4.1	17.0	7.4	2.9
	BE	18 800	0.073	3.0	30.9	2.4	2.1
	THF	15 750	0.096	9.6	9.4	1.0	1.7
	BN	14 150	0.014	2.8	35.2	0.50	1.5

[a] Scatter of results: $\pm 100-150$ cm^{-1}. [b] Error is about 10%. Thus the maximum error is about 20% for the rate constants k_f and k_{nr} and about 10% for the transition moment M_{flu}.

Table 3. Slopes of the Solvatochromic Plots of the CT Absorption (eq 1), CT Fluorescence (eq 2a) and Stokes Shift (eq 3 Properly Modified According to the McRae Model[62]) of the 9-Acridyl Derivatives of Aromatic Amines

compd	$\vec{\mu}_g(\vec{\mu}_e-\vec{\mu}_g)a_o^3$,[a] eV	$\vec{\mu}_e(\vec{\mu}_e-\vec{\mu}_g)/a_o^3$,[a] eV	$(\vec{\mu}_e-\vec{\mu}_g)^2/a_o^3$,[b] eV
BJ	0.35	2.03	0.62
BDMA	0.35	2.05	0.61
BTMP		2.02	
BDMT		2.07	
BDMR		2.08	
BTMA		2.10	
BDMN		1.98	

[a] Data in polar solvents (from ethyl ether to acetonitrile) with solvent polarity function $f(\epsilon) - 0.5f(n)$ (eq 2b) corresponding to the Lippert−Mataga model.[56] [b] Data in the whole range of the solvents with the use of the McRae solvent polarity function $F(\epsilon) - F(n)$ (eq 4c).

$$^1\Psi_{CT} \approx c_1\Phi_{CT} + c_2\Phi_{L_a} \quad \text{with} \quad c_1^2 + c_2^2 = 1 \qquad (5)$$

(in the above expression the relatively small contribution of the ground-state configuration is neglected). The symmetry-allowed mixing of the lowest ^{1}CT state with the intense ^1L_a excitation in the acridyl or anthryl subunit (these excited singlet states are the nearest ones in energy) leads to a lowering of the charge transfer state energy with respect to a "pure" ^{1}CT state because of a stabilizing character of such interactions. For the same energy of the interacting states one can obtain $c_1 = c_2 = (1/2)^{1/2}$. The increasing energy gap between the ^{1}CT and ^1L_a states results in the lowering of the ratio c_2/c_1 (with $c_2 \rightarrow 0$ and $c_1 \rightarrow 1$). Thus, the correct analysis of the solvatochromic effects on the radiative charge transfer transitions should include the variation of the dipole moment μ_e induced by the change of the excited state electronic structure depending on the energy gap between the interacting ^{1}CT and ^1L_a states. Accidentally, for the 9-anthryl and 9-acridyl derivatives of aromatic amines this effect can be described[28] in terms of the model proposed by McRae, although eqs 4a−c assume too large of a polarizability value $\alpha/a_o^3 = 0.5$ (which corresponds to the value of the refractive index of a solute as large as $n \cong 2$). It is due to the fact that the use of the solvent polarity function expressed by eq 4c {i.e., $F(\epsilon) - 0.5F(n)$} leads to the values of the excited-state dipole moments μ_e in a nonpolar environment of about $(1/2)^{1/2}$ times smaller than those related to highly polar solvents (cf., refs 28a and 57).

3.3. Electronic Coupling Elements V_0 and V_1. In order to gain more insight into the changes of the electronic structure and molecular conformation accompanying the excited-state electron transfer we have compared the probabilities of the radiative transitions corresponding to the CT absorption and CT emission in various solvents. The solvent dependence of the radiative rate constants and related electronic transition dipole moments allows us, according to the following procedures, to obtain the electronic matrix elements V_0 and V_1 describing the electronic coupling between the lowest excited charge transfer state ^{1}CT and the ground state S_0 or the locally excited ^{1}LE state of suitable symmetry lying most closely in energy, respectively.

3.3.1. Analysis of the CT Absorption Spectra. The transition dipole moment M_{abs} corresponding to the $^1\text{CT} \leftarrow S_0$ absorption can be determined from an approximate expression[63,64]

(63) Birks, J. B. In *Photophysics of Aromatic Molecules*; Wiley: New York, 1978; p 51.
(64) Michl, J.; Thulstrup, E. W. In *Spectroscopy with Polarized Light*; VCH: New York, 1986; pp 28 and 75.

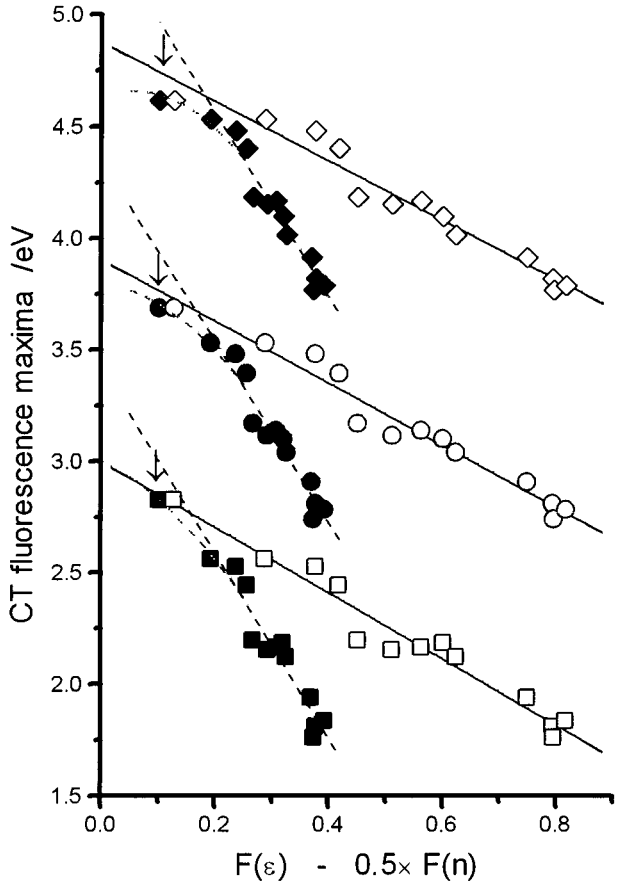

Figure 8. Solvatochromic shift of the energy related to the CT flurescence maxima for BDMA (squares), BTMP (circles), and BDMR (diamonds) as a function of solvent polarity corresponding to the Lippert−Mataga model[56] (eq 2a, full signs) or the model proposed by Mc Rae[62] (eq 4b, open signs). The arrow indicates the deviation in nonpolar medium (methylcyclohexane) from the linear correlation observed in polar solvents (ethyl ether, butyl acetate, ethyl acetate, tetrahydrofuran, 1,2-dichloroethane, 1,2-dichloromethane, butyronitrile, *N*,*N*-dimethylformamide, acetonitrile, and dimethyl sulfoxide) using the Lippert−Mataga solvent polarity function (eq 2b). Correlations for BTMP and BDMR are shifted along the *y*-axis by a factor of 1 and 2 eV, respectively.

$$|M_{abs}|^2 = \frac{3 \ln 10}{8\pi^3 N_A} \frac{hc}{n\tilde{\nu}_{abs}^{CT}} \int_{band} \epsilon(\tilde{\nu})\, d\tilde{\nu} \qquad (6)$$

where $\epsilon(\tilde{\nu})$ denotes the molar CT absorption coefficient at wavenumber $\tilde{\nu}$; h, c, and N_A are Planck constant, the speed of light, and Avogadro number, respectively.

The values of M_{abs} for 9-acridyl derivatives of aromatic amines have been estimated by means of a procedure which decomposes the total low-energy absorption spectrum into the individual transitions ^{1}CT ← S_0 and $^1(\pi,\pi^*)$ ← S_0 (the application of this procedure for BDMR and BTMP is illustrated in Figure 4). The separation is based on a mirror relationship between the reduced CT absorption band (as plotted in the form $\epsilon(\tilde{\nu})/\tilde{\nu}$ vs $\tilde{\nu}$) and the reduced CT fluorescence spectrum (i.e., a plot of the emission intensity $I(\tilde{\nu}_f)/\tilde{\nu}_f^3$ vs $\tilde{\nu}_f$). This relationship has been recently observed for the D−A derivatives of carbazole containing various dicyanobenzenes as electron acceptors[13] and for BJ.[22] The procedure was applied for all the molecules studied, but the separation is less reliable especially for BDMN and BTMA (because of the significant overlap between the CT band and the $^1(\pi,\pi^*)$ ← S_0 transitions localized in the acridyl moiety) than that for BJ and BDMA (Figures 4 and 5). The estimated M_{abs} values for all the *p*-acridyl derivatives of aromatic amines in THF are collected in Table 1; they vary from about 1 D for BDMN to 2.5 D (BJ) and 2.7 D (BDMA). For BJ, the M_{abs} values have been found[22] to be constant (with uncertainty of about ±0.2 D) over the whole solvent range.

The quantitative analysis of the absorption spectra shows that the appearance of the ^{1}CT ← S_0 band in the D−A acridine derivatives generates a significant decrease of the intensity of the band corresponding to the $^1(\pi,\pi^*)$ ← S_0 excitations localized in the acceptor (i.e., acridine) subunit. The increase of the value of the molar extinction coefficient $\epsilon(\tilde{\nu}_{abs}^{CT})$ at the CT absorption band maximum is related to the decrease of $\epsilon(\tilde{\nu})_{LE}$ which corresponds to the maximum of the band dominated by the ^1L_a ← S_0 transition (Table 1). For BDMN the appearance of a weak shoulder corresponding to the ^{1}CT ← S_0 transition results in a very small change of the intensity of the ^1L_a ← S_o excitation with respect to that in acridine. On the other hand, for BJ, BDMP, and BDMA which show the relatively intense CT absorption band, the intensity of the band related to the ^1L_a ← S_o excitation is about 30−40% smaller than that of acridine. Similar effects have been observed for AJ and ADMA.[22] It indicates that for a quantitative description of the transition dipole moments we have to apply the Murrell concept[33] of the three-state model which considers the symmetry-allowed mixing of the ^{1}CT state with the intense ^{1}LE transition lying most closely in energy.

The wave functions of the ground state (S_0), the excited charge transfer state (^{1}CT), and the locally excited state (in the case of the D−A acridine and anthracene derivatives it is the ^1L_a state related to the acceptor subunit) can be expressed as follows

$$^1\Psi_{S_0} \approx g_1\Phi_{S_0} + g_2\Phi_{^1CT} \quad \text{with} \quad g_1^2 + g_2^2 = 1 \qquad (7a)$$

$$^1\Psi_{CT} \approx c_1\Phi_{^1CT} + c_2\Phi_{^1L_a} - c_3\Phi_{S_0} \quad \text{with} \quad c_1^2 + c_2^2 + c_3^2 = 1 \qquad (7b)$$

$$^1\Psi_{L_a} \approx e_1\Phi_{^1L_a} - e_2\Phi_{^1CT} \quad \text{with} \quad e_1^2 + e_2^2 = 1 \qquad (7c)$$

To analyze the absorption spectra, the wave functions of the Franck−Condon ^{1}CT(a) state reached in absorption and the ^1L_a state can be approximated as $c_1 \approx e_1$, $c_2 \approx e_2$, $c_3 \ll c_1, c_2$. This approach neglects the relatively small contribution of the ground-state configuration to the wave function $^1\Psi_{CT}$ (which is reasonable because of the one order of magnitude larger energy gap between these excited states and the ground state than that between ^{1}CT(a) and ^1L_a states). Consequently, the values of c_1 and $c_2 = (1-c_1)^{1/2}$ can be estimated from the change of the intensity of the absorption band corresponding to the ^1L_a ← S_0 transition in the 9-acridyl derivatives of aromatic amines ($\epsilon(\tilde{\nu})_{LE}$) with respect to that in acridine[51,52b] and 9-phenylacridine[52b] ($\epsilon(\tilde{\nu})_{ref} = 12600 \pm 300$ M^{-1} cm^{-1})

$$c_1^2 \approx \epsilon(\tilde{\nu})_{LE}/\epsilon(\tilde{\nu})_{ref} \qquad (8)$$

where $\epsilon(\tilde{\nu})_{LE}$ and $\epsilon(\tilde{\nu})_{ref}$ denote the molar absorption coefficients at the spectral position of the maximum of the most intense vibronic band of the ^1L_a ← S_0 transition (Figures 4 and 5). The ratio of c_1 and c_2 is related to the electronic coupling element V_{1A} between the ^{1}CT(a) and ^1L_a states

$$V_{1A} \approx (c_2/c_1)(E_{LE}^A - hc\tilde{\nu}_{abs}^{CT}) \qquad (9)$$

where E_{LE}^A is the ^1L_a state energy.

Thus, the analysis of the absorption bands corresponding to the $^1CT \leftarrow S_0$ and $^1L_a \leftarrow S_o$ transitions should yield the values of the interaction elements V_{1A}. The results collected in Table 4 were obtained from the two latter equations with $E^A_{LE} = 3.25$-($\pm$0.05) eV;[51,52] they vary between $V_{1A} = 0.21(\pm 0.03)$ eV (BJ) to about 0.02 − 0.04 eV (BDMN). The contribution resulting from the borrowing mechanism to the intensity of the CT absorption band is given by a product $c_2M^A_{LE}$, where M^A_{LE} denotes the transition dipole moment value corresponding to the radiative transition $^1L_a \leftarrow S_o$ in acridine ($M^A_{LE} = 2.4 \pm 0.2$ D was evaluated from the respective absorption spectra[51,52,65]). It leads to the values of $c_2M^A_{LE}$ being about 1.5−2.0 times smaller than the experimental M_{abs} values (Table 1). It seems real to relate this difference to the direct interactions between the $^1CT(a)$ state and the ground state[34] The first term in the

$$M_{abs} \approx c_1V_{0A}(\mu_e - \mu_g)/hc\tilde{\nu}^{CT}_{abs} + c_2M^A_{LE} \qquad (10)$$

above equation corresponds to the Mulliken two-state model;[16] the second one represents the Murrell borrowing mechanism[33] (the relation assumes that the linear combination coefficient g_1 in eq 7a is close to unity). It should be noted that for c_1 approaching unity, eq 10 together with eq 9 lead to the formalism described in refs 20 and 21. Equation 10 allows us to estimate the values of the electronic coupling elements V_{0A} between the $^1CT(a)$ state and the ground state (the results presented in Table 4 were obtained with the value of $\mu_e - \mu_g = 22.5$ D). Because for BDMN and BTMA the transitions $^1CT \leftarrow S_0$ and $^1(\pi,\pi^*) \leftarrow S_0$ are superimposed in the low-energy absorption region (Figure 5), the interaction elements V_{0A} and V_{1A} for these compounds could be only roughly estimated. Due to the same reason, the similar analysis has been performed only for two selected D−A anthracene derivatives: AJ and ADMA. For both compounds the analysis leads to $c_1 \approx c_2$ and $V_{1A} \approx V_{0A}$ {e.g., for AJ in THF solution $V_{1A} \approx V_{0A} \approx 0.14$ ($\pm$0.02) eV}.[22]

It is interesting to note that the values of V_{0A} and V_{1A} are similar one to another for each D−A acridine and anthracene derivative. For a quantitative description of this finding, we have used the concept that the electronic coupling elements are mainly determined by the interactions between the carbon atoms forming A−D bond (the formalism proposed by Dogonadze et al.[66] has been adapted in refs 13 and 22)

$$V_0 = C^A_{LUMO}C^D_{HOMO}\,\beta_{CC}\cos(\Theta_{A-D}) + \text{const} \qquad (11a)$$

$$V^A_1 = C^A_{HOMO}C^D_{HOMO}\,\beta_{CC}\cos(\Theta_{A-D}) + \text{const} \qquad (11b)$$

$$V^D_1 = C^A_{LUMO}C^D_{LUMO}\,\beta_{CC}\cos(\Theta_{A-D}) + \text{const} \qquad (11c)$$

where Θ_{A-D} denotes the angle between the planes of the acceptor and donor subunits; C_{LUMO} and C_{HOMO} are the LCAO coefficients of the $2p_z$ atomic orbitals (where z is the axis perpendicular to the acceptor (A) or donor (D) rings) of the highest occupied molecular orbital (HOMO) and of the lowest unoccupied molecular orbital (LUMO) at the carbon atoms of the A−D bond. β_{CC} is the resonance integral for these atoms. V_0, V^A_1, and V^D_1 are the electronic matrix elements describing the electronic coupling between the lowest excited charge transfer state ^1CT and the ground state S_0 or the locally excited state ^1LE either localized in the acceptor or in the donor, respectively. Expressions 11b and 11c assume that the ^1LE state is mainly described by a configuration corresponding to an electron jump from HOMO to LUMO (which is the case of the lowest ^1L_a states of the studied compounds). The values of Θ^G_{A-D} (which is related to the equilibrated ground-state conformation of the molecules), C_{LUMO}, and C_{HOMO} (for isolated neutral subunits) have been computed by the semiempirical AM1 method. Assuming $\beta_{CC} = 2.30$ eV and neglecting the electronic interactions between the remaining pairs of atoms in the donor−acceptor systems (i.e., const = 0 eV), the values of V_0(calc) and V^A_1(calc) for the D−A acridine derivatives have been calculated from eqs 11a and 11b, respectively. It is shown in Table 4 that these values agree well with the experimental ones V_{0A} and V_{1A}; the corresponding correlation is presented in Figure 9.

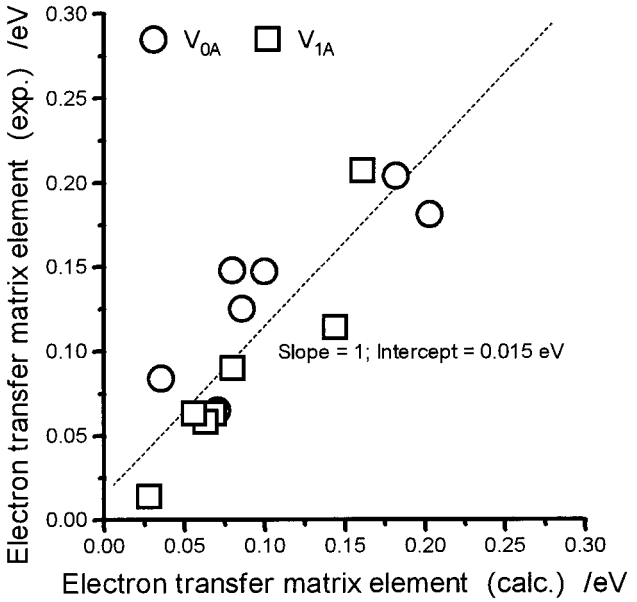

Figure 9. Correlation (for the 9-acridyl derivatives of aromatic amines) between the electronic matrix elements describing the electronic coupling between the lowest excited charge transfer ^1CT state and the ground state S_0 (V_{0A}) or the locally excited ^1L_a state (V_{1A}) (as estimated from the experimental electronic transition dipole moments of the CT absorption with the use of eqs 6 and 8−10) and the electronic coupling elements calculated from the relations 11a and 11b.

3.3.2. Analysis of the Radiative Charge Recombination $^1CT \rightarrow S_0$. The electronic coupling elements V_0 and V_1 can also be estimated from the CT fluorescence investigations. Applying a simple kinetic model of an irreversible excited charge transfer state formation (with 100% efficiency) the radiationless (k_{nr}) and radiative (k_f) rate constants have been determined from the CT fluorescence quantum yields Φ_f and lifetimes τ

$$k_{nr} = (1 - \Phi_f)/\tau \qquad (12a)$$

$$k_f = \Phi_f/\tau \qquad (12b)$$

and the resulting electronic transition dipole moments M_{flu} are given by[63,64]

$$k_f = \frac{64\pi^4}{3h}(n\tilde{\nu}^{CT}_{flu})^3|M_{flu}|^2 \qquad (12c)$$

An interesting result is provided by the identical dependence of the radiative k_f and nonradiative k_{nr} rate constants (as well as the corresponding M_{flu} values)[67] for related pairs of compounds containing acridyl or anthryl as an electron acceptor (e.g., BJ and AJ, or BDMA and ADMA) on the spectral position of the CT fluorescence maxima (which express the polarity of

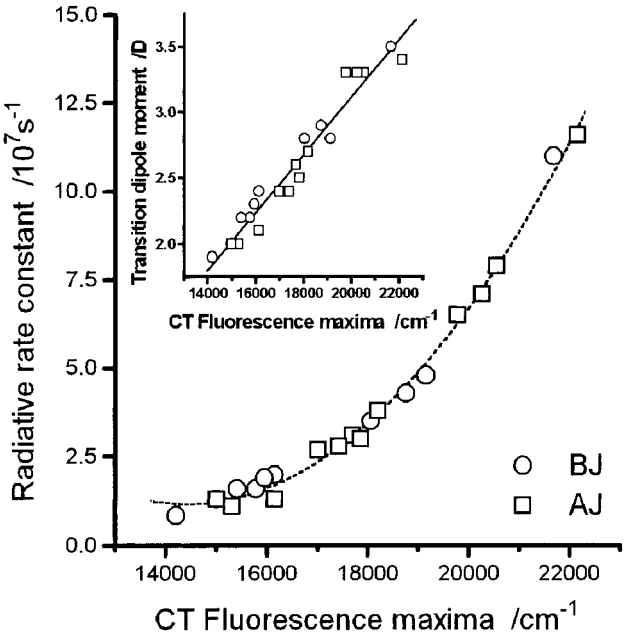

Figure 10. Dependence of the radiative rate constants k_f on the spectral position of the CT fluorescence maxima at room temperature for AJ (squares) and BJ (circles). Insert shows the solvation effects on the transition dipole moments of the CT fluorescence for these compounds. Correlations take into account the whole range of the solvents (see text).

the surrounding medium). This finding (illustrated in Figure 10) indicates the similar photophysical properties of both groups of D−A molecules; the differences in thermodynamics and kinetics of the photoinduced electron transfer seem to be induced mainly by the larger electron affinity of the acridyl subunit than that of the anthryl moiety.

The values of M_{flu} for the D−A acridine derivatives (Table 2), similarly as for other aryl derivatives of aromatic amines,[28] and contrary to *N*-carbazoyl derivatives of aromatic nitriles,[13,32] decrease significantly with increasing solvent polarity. It suggests[20] that the electronic transition dipole moments M_{flu}, analogously to M_{abs} (eq 10), are determined not only by the direct interactions between the solvent-equilibrated fluorescent ^{1}CT(f) state and the Franck−Condon ground state but also the contribution from the locally excited configuration should be taken into account

$$M_{flu} \approx c_1 V_{0F}(\mu_e - \mu_g)/hc\tilde{\nu}_{flu}^{CT} + c_2 M_{LE}^{A} \qquad (13)$$

where V_{0F} denotes the electronic coupling elements between the ^{1}CT(f) state and the ground state. It should be noted, however, that without additional assumptions the fluorescence studies do not allow us to determine V_{0F} and V_{1F} (which is related to the interactions between the ^{1}CT(f) and ^1L_a states). The situation is considerably simplified in highly polar environment. Due to the increasing energy gap between the ^{1}CT(f) state and ^{1}LE state(s) as well as the lowering of the transition energy $hc\tilde{\nu}_{flu}^{CT}$, the M_{flu} values can be approximated applying the two-state model,[16] i.e., the dominant electronic coupling between the ^{1}CT(f) and S_0 states. Neglecting the second term in eq 13 and assuming that the value of c_1 is close to unity, the interaction elements V_{0F} for all the D−A acridine derivatives in butyronitrile could be estimated from the first term in eq 13. The values of V_{0F}, collected in Table 5, are similar to those (V_{0A}) obtained from the CT absorption analysis. This finding seems to indicate that in highly polar media the compounds do not undergo any significant conformational changes (e.g., related to the angle Θ_{A-D} between the planes of the donor and acceptor subunits) accompanying the excited-state charge separation. A similar analysis has been performed for selected D−A anthryl derivatives (AJ, ADMA, and 4-(9-anthryl)-3,*N*,*N*-trimethylaniline (ADMT), 4-(9-anthryl)-3,5,*N*,*N*-tetramethylaniline (ATMA), and 4-(9-anthryl)-*N*,*N*-dimethyl-1-naphthylamine (ADMN). The analysis leads to the very similar values of the interaction elements V_{0F} in highly polar solvents (BN and ACN) to those obtained for the corresponding acridine derivatives (Table 5).

In low polarity media, however, the situation is quite different. Undoubtedly, an important result is the finding that the transition dipole moments corresponding to the CT fluorescence are larger than those representing the CT absorption (i.e., $M_{flu} > M_{abs}$, cf. Tables 1 and 2). This fact can hardly be explained by the variations of the c_1 and c_2 coefficients (relation 7b) arising simply from the changes of the respective energy gaps. On the contrary, the opposite effect is expected because of the increase of the energy gap between the ^{1}CT(f) and ^1L_a states. Most probably the increase of the electronic coupling elements V_{0F} and/or V_{1F} (with respect to V_{0A} and/or V_{1A}) is responsible for the observed effects. In order to estimate the interaction elements two limiting cases are of interest. The first one is based on the assumption $c_1 = c_2 = (1/2)^{1/2}$. It leads[22] to the upper limit of $V_{1F} \approx 0.60$ eV for BJ in MCH and $V_{1F} \approx 0.55$ eV for AJ in MCH (as estimated from eq 9 properly modified for the CT fluorescence) as well as to the lower limit of $V_{0F} \approx 0.30$ eV for both compounds (with $M_{LE}^{A} = 2.4$ D[51,52,65] and the use of eq 13).

The second approach assumes that both electronic coupling elements are similar as it has been found from the analysis of the absorption spectra. It leads to the values of interaction elements $V_{0F} \approx V_{1F}$ presented in Table 5, which are about twice the corresponding V_{1A} or V_{0A} values. It is noteworthy that the values of V_{0F} and V_{1F} for all the D−A acridyl derivatives and for selected D−A compounds containing anthryl as an acceptor moiety monotonically decrease with increasing solvent polarity to the corresponding V_{0A} and V_{1A} values characteristic for the CT absorption (as obtained from eqs 6 and 8−10). These effects most probably result from the conformational changes generated by the changes of the strength of the coupling between the ^{1}CT(f) and ^1L_a states, which depend on the respective energy gap. Thus, the enlargement of the interaction elements V_{0F} and V_{1F} (with respect to V_{0A} and V_{1A}) should be especially pronounced in the D−A systems with a relatively small energy difference between these states (e.g., ADMA and BDMA). It is in agreement with the results previously obtained by Mataga et al.;[18c] the authors found the values $V_{0F} \approx V_{1F} \approx 0.30-0.40$ eV for the fluorescent ^{1}CT(f) state of ADMA.

The increase of the electronic coupling elements between the solvent-equilibrated fluorescent ^{1}CT(f) state and the ground state as well as between the ^{1}CT(f) state and locally excited state(s) with respect to those corresponding to the Franck−Condon ^{1}CT(a) state (i.e. $V_{0F} \approx V_{1F} > V_{0A} \approx V_{1A}$) suggests that the excited-state charge separation in 9-acridyl and 9-anthryl derivatives of aromatic amines in low polarity solvents is related to the conformational changes resulting in the more planar structure of these compounds. Following the formalism proposed by Dogonadze et al.,[66] we could obtain the dihedral angles Θ_{A-D}^{F} in the fluorescent ^{1}CT(f) state from the expressions 11a and 11b. For example,[22] for AJ and BJ in MCH the values of

(65) Berlman, I. B. *Handbook of Fluorescence Spectra of Aromatic Molecules*; Academic Press: New York, 1971; p 159.

(66) Dogonadze, R. R.; Kuznetsov, A. M.; Marsagishvili, T. A. *Electrochim. Acta* **1980**, *25*, 1.

Table 4. Experimental[a] (V_{0A} and V_{1A}) and Calculated[b] {V_0(calc) and V_1^A(calc)} Values of Electronic Matrix Elements Describing the Electronic Coupling between the ^{1}CT State and the Ground State {V_{0A} and V_0(calc)} or the Locally Excited ^{1}LE State Related to the Acceptor Subunit {V_{1A} and V_1^A(calc)} for the D−A Acridine Derivatives[f]

compd	V_{0A},[a] eV	V_{1A},[a] eV	Θ^G_{A-D},[c] deg	C^D_{HOMO}	V_0(calc)[b] eV	V_1^A(calc),[b] eV
BJ	0.18	0.21	64	0.42	0.20	0.16
BDMA	0.20	0.12	68	0.44	0.18	0.14
BTMP	∼0.15	∼0.09	80	0.48	0.09	0.07
BDMT	∼0.12	∼0.06	80	0.45	0.09	0.07
BDMR	∼0.15	∼0.06	82	0.52	0.08	0.06
BTMA	∼0.06	∼0.06	82	0.46	0.07	0.06
BDMN	≈0.08	≈0.02	84	0.31[e]	0.04	0.03

[a] Values of V_{0A} and V_{1A} were obtained from the absorption data (Table 1) with the use of Eqs 6 and 8−10. [b] V_0(calc) and V_1^A(calc) were calculated from eqs 11a and 11b, respectively. [c] Θ^G_{A-D} is related to the equilibrated ground-state conformation of the molecule. [d] C^D_{HOMO}, C^A_{HOMO}, and C^A_{LUMO} are the LCAO coefficients (calculated for the isolated chromophores, i.e., for acridine - A or the respective aromatic amine - D) of the $2p_z$ atomic orbitals of HOMO and LUMO at the carbon atoms forming A−D bond. [e] This value corresponds to the twisted ground-state conformation of neutral *N*,*N*-dimethyl-1-naphthylamine. Its radical cation is more planar and the corresponding $C^D_{HOMO} = 0.48$ (which results in the higher value of V_0(calc) = 0.055eV). [f] The values of Θ^G_{A-D}[c] and C^D_{HOMO},[d] C^A_{HOMO}[d] = 0.38, and C^A_{LUMO}[d] = 0.48 were calculated by the AM1 method.

Table 5. Comparison between the Electronic Matrix Elements Describing the Electronic Coupling between the ^{1}CT State and the Ground State Obtained from the Absorption[a] (V_{0A}) and CT Fluorescence[b] (V_{0F}) Investigations for the 9-Acridyl and 9-Anthryl Derivatives of Aromatic Amines (Donors) in the Solvents of Different Polarity: Methylcyclohexane (MCH), Tetrahydrofuran (THF), Butyronitrile (BN), and Acetonitrile (ACN)

acceptor	acridine			anthracene		
donor/solvent	THF V_{0A},[a] eV	BN V_{0F},[b] eV	MCH V_{0F},[c] eV	BN V_{0F},[b] eV	ACN V_{0F},[b] eV	MCH V_{0F},[c] eV
J	0.18	0.15	0.32	0.17[d]	0.16	0.31
DMA	0.20	0.22	0.31	0.21	0.17	0.36
TMP	∼0.15	0.16	0.34			
DMT	∼0.12	0.14	0.26	0.17	0.10	
DMR	∼0.15	0.14	0.23			
TMA	∼0.06	0.10	0.16	0.08	0.10	
DMN	≈0.08	0.12	0.25	0.10		

[a] Values of V_{0A} were obtained from the absorption data (Table 1) with the use of eqs 6 and 8−10. [b] In highly polar solvents the values of V_{0F} were estimated from the first term in eq 13. [c] As estimated from eq 13 assuming $V_{0F} \approx V_{1F}$. [d] Value of $V_{0A} \approx 0.16$ eV has been found for AJ in THF (cf. ref 22).

Θ^F_{A-D} could be found as 45−50° which are about 15−20° lower than those of the angle Θ^G_{A-D} (Table 4). The difference $\Theta^G_{A-D} - \Theta^F_{A-D}$ becomes smaller with increasing solvent polarity, indicating solvent dependence of the fluorescent ^{1}CT(f) state conformation. The other studied compounds show similar behavior.

The dependence of the conformation of aryl derivatives of aromatic amines in the fluorescent ^{1}CT(f) state on solvation can be explained in terms of a simple model assuming two competitive modes of interactions: (i) the Coulombic stabilization of the highly polar ^{1}CT state by a polar surrounding (it could lead to the mutually perpendicular conformation of the D−A system resulting from the large dipole moment of the orthogonal TICT state[26]) and (ii) the stabilization effects related to the interactions between the lowest excited charge transfer state ^{1}CT(f) and the locally excited ^1L_a states (it could result in the more planar conformation of the D−A system due to the increase of the electronic coupling elements V_1^A and/or V_1^D, cf. eqs 11b and 11c, respectively). In the compounds studied the latter effect is expected to be predominant in a low-polarity environment (because of the relatively small energy gap between the ^{1}CT and ^{1}LE states and a small solvation energy) what leads to the more planar conformation in the excited CT state than that in the ground state. In highly polar solvents, hovewer, the relatively strong solute−solvent interactions prevent the flattening of the excited D−A molecule.

3.4. Analysis of the CT Fluorescence Profiles. The analysis of the CT absorption and fluorescence spectra of the D−A acridine and anthracene derivatives indicates solvent-dependent changes of the excited-state solute conformation with respect to that in the ground state. These effects should be reflected by the changes of the band-shape of the CT fluorescence (as being the radiative charge recombination). Theoretical treatments of the rates of electron transfer reactions were described by Marcus.[68] Marcus original theory was derived using classical mechanics; more recent theories take quantum effects into account.[3] The reactions are described using a Golden rule expression in which the rate is given as the product of an electronic coupling element squared (V^2) and a Franck−Condon weighted density of states. The energetic and nuclear parameters of the Franck−Condon factor can be estimated from a band-shape analysis of the charge transfer radiative transitions. Pursuing the analogy between optical spectroscopy of the CT states and thermal electron transfer processes the following expression for the CT fluorescence profile can be obtained[5,11,12]

$$\frac{I(\tilde{\nu}_f)}{n^3\tilde{\nu}_f^{\,3}} = \frac{64\pi^4}{3h}M_{flu}^2\sum_{j=1}^{\infty}\frac{e^{-S}S^j}{j!}\sqrt{\frac{1}{4\pi\lambda_o k_B T}}\times \exp\left[-\frac{(jh\nu_i + \lambda_o + hc\tilde{\nu}_f + \Delta G_{CT})^2}{4\lambda_o RT}\right] \quad (14a)$$

with S being the electron-vibration coupling constant

(67) Values of the radiative rate constants k_f and corresponding transition dipole moments M_{flu} are somewhat higher than those reported previously by us in ref 28a. The discrepancy was caused by the slightly shifted wavelength scale of the excitation monochromator of our spectrofluorimeter. The conclusions presented in ref 28a, however, are still valid.

(68) (a) Marcus, R. A. *J. Chem. Phys.* **1956**, *24*, 966. (b) Marcus, R. A. *Annu. Rev. Phys. Chem.* **1964**, *15*, 155.

$$S = \lambda_i/h\nu_i \quad (14b)$$

and where M_{flu} may principally depend on the wavenumber $\tilde{\nu}_f$ of the emission ($hc\tilde{\nu}_f$ is the energy of the emitted photon), ΔG_{CT} denotes the free energy of the charge recombination process, k_B is the Boltzmann constant, and T labels temperature. λ_o and λ_i denote the reorganization energies in the solute−solvent supermolecule undergoing electron transfer. The reorganization energy λ_o is related to the low-frequency motions such as reorientation of the solvent shell (the outer reorganization energy λ_s) as well as any other low-frequency ($\tilde{\nu}_L$ <200 cm^{-1}) and medium-frequency ($\tilde{\nu}_M \cong 300-600$ cm^{-1})[12,13] nuclear motions of the solute ($\delta\lambda_o$). The inner reorganization energy λ_i corresponds to the high-frequency motions (represented by a single "averaged" mode ν_i) associated with the changes in the solute bond lengths and angles. In low and medium polarity solvents the quantities relevant for the electron transfer (i.e., ΔG_{CT}, $h\nu_i$, λ_i, and λ_o) have been estimated by means of the fitting procedure (as described previously in refs 12 and 13) concerning the variation of all the parameters. For the 9-acridyl derivatives of aromatic amines in these media the $h\nu_i$ values (being about 0.16(±0.01) eV for the derivatives of *N*,*N*-dimethylanilines and 0.17(±0.02) eV for BDMN) have been found to be nearly constant within the accuracy of the fit. In highly polar solvents, however, because of the large broadening of the partially recorded CT fluorescence spectra (cf. Figure 11, the long-wave threshold of our spectrofluorimeter is 800 nm) the procedure was simplified by fixing $h\nu_i$ at the average value in medium polarity media. Taking into account the dependence of the electronic transition dipole moment M_{flu} on the emitted photon energy (cf. Table 2) does not influence significantly the computational results. It is noteworthy that similar results are obtained in the analyses considering the dependence of the fluorescence intensity $I(\tilde{\nu}_f)$ on $\tilde{\nu}_f^3$ or $\tilde{\nu}_f$ (cf. also refs 12 and 13). Representative examples of the numerical fits (within a single high-frequency mode approximation according to eq 14) of the CT fluorescence spectra are presented in Figure 11; the experimental emission profiles of all the D−A compounds studied in the whole range of the solvents could be adequately reproduced. It should be noted, however, that ΔG_{CT} and λ_o as well as $h\nu_i$ and λ_i turn out to be somewhat correlated, leading to a numerical uncertainty of their values of about ±0.02 eV (because of the model approximations the real uncertainty may be somewhat larger).

The values of ΔG_{CT} and λ_o extracted from the analysis of the profiles of the reduced CT fluorescence spectra (i.e., a plot of the ratio $I(\tilde{\nu}_f)/\tilde{\nu}_f^3$ vs $\tilde{\nu}_f$, eq 14a) depend on the solvent polarity, as expected (Figures 12 and 13). The more polar is the medium, the smaller is the energy gap between the ground state and the excited ^{1}CT state and the larger is the outer reorganization energy λ_s, in agreement with the continuum dielectric model of solvation. An analysis of the solvent effects on λ_o is possible according to the following expression[13,28,69]

$$\lambda_o \cong \delta\lambda_o + \lambda_s = \delta\lambda_o + \frac{(\vec{\mu}_e - \vec{\mu}_g)^2}{a^3_o}[F'(\epsilon) - F'(n)] \quad (15)$$

where $F'(\epsilon) - F'(n)$ corresponds either to the Lippert−Mataga (eq 2b) or to the McRae (eq 4c) solvent polarity function. This relation is different from the classical Marcus expression,[70] but it is more suitable for the direct comparison with the results of the investigations of the solvatochromic effects on the spectral position of the CT fluorescence maxima and Stokes shift (Table 3). Similarly to the solvent effects on the CT fluorescence, in the low polarity solvents a deviation from the linear relationship between the reorganization energy λ_o and the Lippert−Mataga solvent polarity function is observed. The linear correlation is obtained with the function proposed by McRae; the representative results for BDMA, BTMP, and BDMR are shown in Figure 12. The value of $(\vec{\mu}_e - \vec{\mu}_g)^2/a_o^3 \approx 0.76$ eV obtained from the mean slope of the plots corresponding to eq 15 agree well with those collected in Table 3. The intercept of the averaged plot,

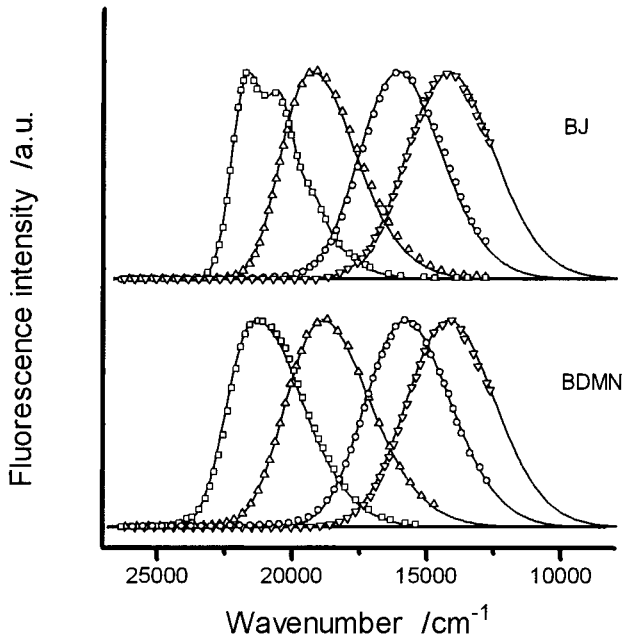

Figure 11. Room temperature CT fluorescence spectra of BDMN and BJ in methylcyclohexane, butyl ether, tetrahydrofuran, and butyronitrile (from left to right, respectively) and the corresponding numerical fits (solid lines) using eqs 14a and 14b.

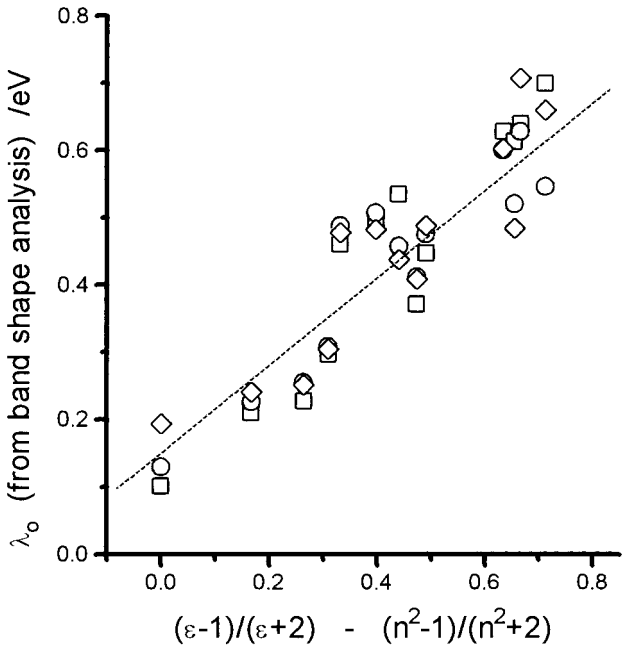

Figure 12. Dependence (corresponding to eq 15) of the reorganization energy λ_o related to the low-freqency solvent and solute motions accompanying the excited-state electron transfer on the solvent polarity function F(ϵ) − F(n) (eq 4c) for BDMA (squares), BTMP (circles), and BDMR (diamonds). Correlation takes into account the whole range of the solvents (see text).

(69) Bader, J. S.; Berne, B.J. *J. Chem. Phys.* **1996**, *104*, 1293.
(70) Marcus, R. A. *J. Chem. Phys.* **1965**, *43*, 679.

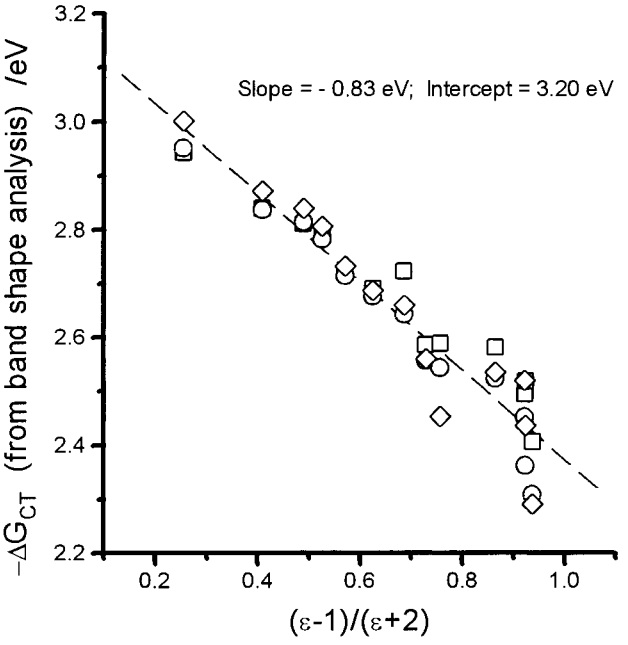

Figure 13. Dependence of the free energy of the charge recombination process ΔG_{CT} on the solvent polarity function F(ϵ), resulting from the model proposed by McRae (eq 4c), for BDMA (squares), BDMT (circles), and BDMR (diamonds). The slope is related to the value of $(\vec{\mu}_e^2-\vec{\mu}_g^2)/a_o^3$. Correlation takes into account the whole range of the solvents (see text).

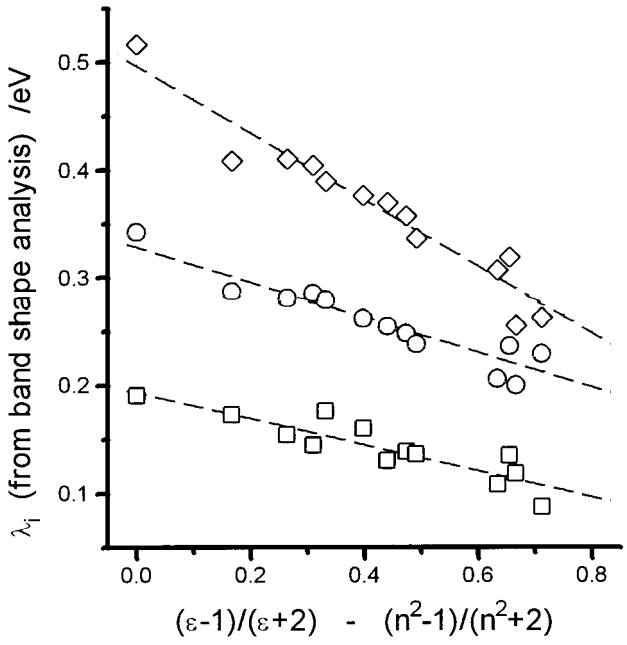

Figure 14. Dependence of the inner reorganization energy λ_i corresponding to the high-frequency motions related to the changes in the solute bond lengths and angles accompanying the excited-state electron transfer on the solvent polarity function F(ϵ) − F(n) (eq 4c) for BDMA (squares), BTMP (circles), and BDMR (diamonds). Correlations take into account the whole range of the solvents (see text). Plots for BTMP and BDMR are shifted along the *y*-axis by a factor of 0.1 and 0.2 eV, respectively.

being about $\delta \approx 0.1$ eV, may be related to the contribution of low-frequency (e.g., associated with librations, internal rotations) and/or medium-frequency ($\tilde{\nu}_M = 300-500$ cm^{-1})[12,13] nuclear motions of the solute. Another possible explanation of the nonzero intercept value may be be related to the breakdown of the Marcus formalism in the low polarity solvents.[71]

An unexpected result is provided by the solvent effects on the inner reorganization energy λ_i related to the changes in the solute bond lengths and angles accompanying excited-state electron transfer. Contrary to the previous reports on a variety of compounds,[5−13,28b] where it has been found (or assumed) that for a particular D−A molecule the quantities λ_i and $h\nu_i$ did not depend on the solvent properties, 9-acridyl derivatives of aromatic amines show a significant decrease of λ_i with increasing solvent polarity (Figure 14). It is noteworthy that this effect is the most pronounced for BDMR, and it is also larger for BTMP than for the other D−A acridine derivatives. It suggests that the interpretation of this finding should take into account the increase of the A−D bond order upon intramolecular excited-state charge separation (Figure 15). The order of this bond depends on the compound, and for a particular molecule it can be correlated with the mutual conformation of the donor and acceptor subunits (e.g., with the value of the angle Θ_{A-D} between the planes of the donor and acceptor subunits). The decrease of λ_i with solvation energy most probably reflects the inseparability between the low frequency nuclear motions of a solute (e.g., associated with the torsion around the A−D bond) and the changes of the A−D bond length and the respective angles.[72] In low polarity solvents the excited-state electron transfer leads to the more planar conformation and to the increase of the A−D bond order with respect to that in the ground state; it results in the relatively high values of λ_i. On the other hand, in polar solvents the lack of any significant change of the molecular structure accompanying the excited-state charge separation leads to the small values of λ_i.

An independent verification of the computed parameters is possible due to the following approximate expressions for the maxima of the reduced CT absorption and fluorescence spectra[5−13]

$$hc\tilde{\nu}_{abs}^{CT} \approx -\Delta G_{CT} + \lambda_o + \lambda_i \quad (16)$$

$$hc\tilde{\nu}_{flu}^{CT} \approx -\Delta G_{CT} - \lambda_o - \lambda_i \quad (17)$$

Thus, the sum of the CT absorption and fluorescence maxima is simply connected with ΔG_{CT}

$$-\Delta G_{CT} \approx \frac{1}{2}(hc\tilde{\nu}_{abs}^{CT} + hc\tilde{\nu}_{flu}^{CT}) \quad (18)$$

and, correspondingly, their difference with the sum of the reorganization energies

$$hc\tilde{\nu}_{abs}^{CT} - hc\tilde{\nu}_{flu}^{CT} \approx 2(\lambda_o + \lambda_i) \quad (19)$$

Figures 16 and 17 show that the sum of the energies related to the experimental positions of the maxima of the reduced CT absorption and fluorescence spectra as well as the energy of the corresponding Stokes shift agree well with those predicted by the band shape analysis. It should be noted, however, that $\lambda_o + \lambda_i$ in highly polar solvents is slightly larger (about 0.06

(71) (a) Matyushov, D. V.; Schmid, R. *J. Chem. Phys.* **1995**, *103*, 2034. (b) Matyushov, D. V. *Chem. Phys.* **1996**, *211*, 47. (c) Matyushov, D. V.; Schmid, R.; Ladanyi, B. M. *J. Phys. Chem. B* **1997**, *101*, 1035.

(72) Previous investigations[28b] of the solvent effects on the half-width of the CT fluorescence spectra of aryl derivatives of *N*,*N*-dimethylaniline assumed that $\lambda_i h\nu_i$ was constant over a wide range of solvent polarity. With $h\nu_i = 0.2$ eV the values of λ_i have been obtained as small as 0.07(±0.02) eV. On the contrary the analysis led to the significant contribution of the reorganization energy $\delta\lambda_o$ related to the low-frequency nuclear motions (e.g., torsion around the A−D bond) of ATMA, ADMT, and ADMA. The discrepancy with the results of the present analysis arises from the false assumption. The conclusions presented in ref 28b, however, are still valid.

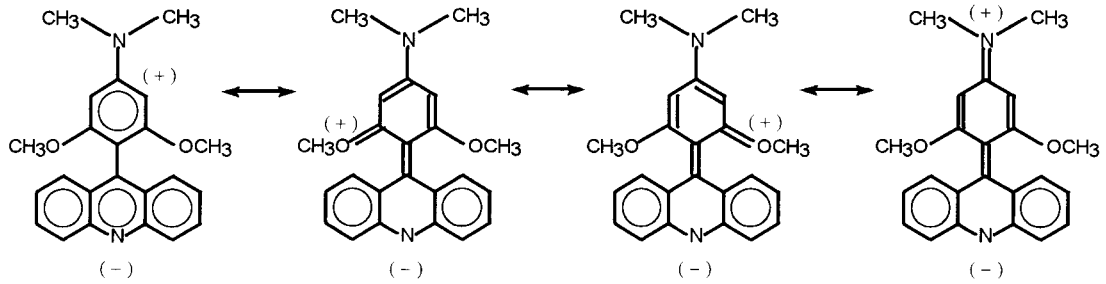

Figure 15. Resonance structures of the zwitterionic forms related to the charge transfer excited state of BDMR as a representative example of 9-acridyl derivatives of aromatic amines.

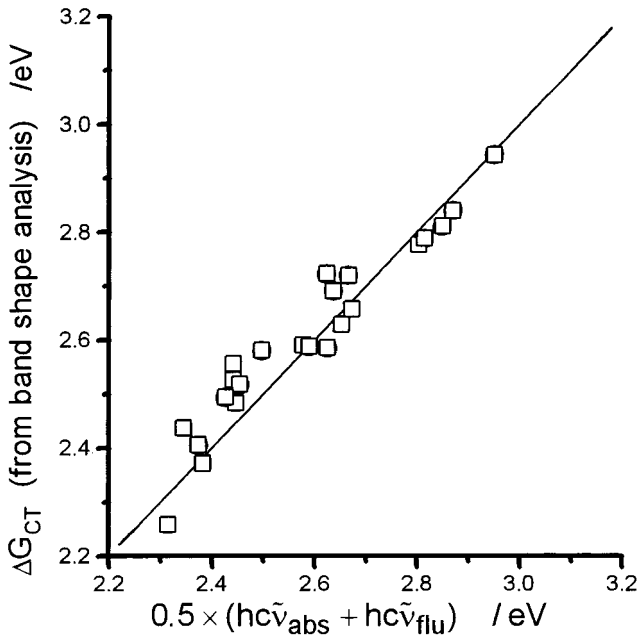

Figure 16. Correlation (related to eq 18) between the free energy of the charge recombination process ΔG_{CT} obtained from the analysis of the reduced CT fluorescence profile (according to eqs 14a and 14b) and the sum of the energies corresponding to the maxima of the reduced CT absorption (as plotted in the form $\epsilon(\tilde{\nu})/\tilde{\nu}$ vs $\tilde{\nu}$) and fluorescence spectra (a plot of the ratio $I(\tilde{\nu}_f)/\tilde{\nu}_f^3$ vs $\tilde{\nu}_f$) for BDMA (circles) and BJ (squares) in the whole range of the solvents (see text).

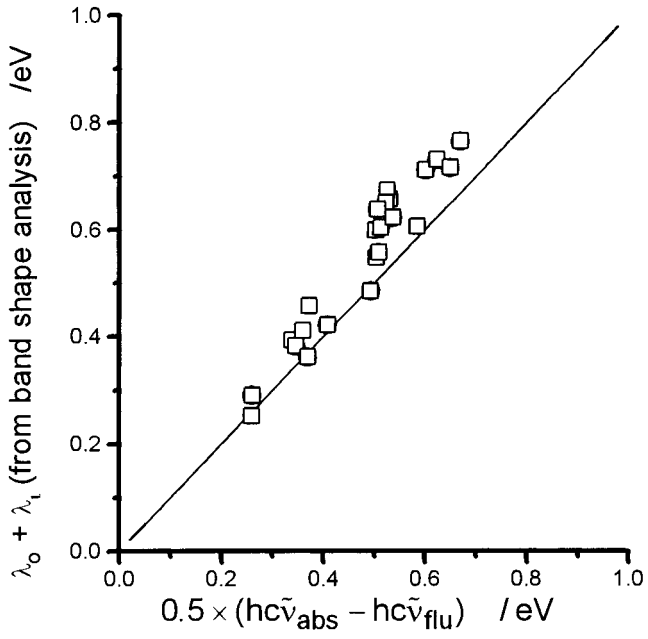

Figure 17. Correlation (related to eq 19) between the sum of the reorganization energies $\lambda_o + \lambda_i$ obtained from the analysis of the reduced CT fluorescence profile (according to eqs 14a and 14b) and the energy corresponding to the Stokes shift between the maxima of the reduced CT absorption (as plotted in the form $\epsilon(\tilde{\nu})/\tilde{\nu}$ vs $\tilde{\nu}$) and fluorescence spectra (a plot of the ratio $I(\tilde{\nu}_f)/\tilde{\nu}_f^3$ vs $\tilde{\nu}_f$) for BDMA (circles) and BJ (squares) in the whole range of the solvents (see text).

eV) than the experimental Stokes shift. The observed deviations—which are within the accuracy of the fitting procedure (ca. 3 × 0.02 eV)—most probably arise from the fact that the applied procedure of the band-shape analysis does not separate the low- and medium-frequency nuclear motions of the solute (cf. refs 12 and 13).

The other verification of the computed data could be possible by the comparison of the experimental radiationless rate constants k_{nr} (Table 2) and the values predicted by the Marcus theory[8,13,73] for the direct radiationless charge recombination processes, DICR (cf. eq 21 in ref 13). The nonradiative depopulation of the lowest excited ^{1}CT state of 9-acridyl and 9-anthryl derivatives of aromatic amines, similarly to *N*-carbazoyl derivatives of aromatic nitriles,[13] is most probably controlled by two competitive mechanisms—an intersystem crossing (ISC) to the triplet manifold and a DICR in the singlet manifold. To examine the latter process it should be recognized to what degree the nonradiative deactivation of the ^{1}CT state can be assigned to the internal conversion (IC) path and how far to the ISC processes (generally, ISC may occur to the charge transfer ^{3}CT triplet state and/or to the locally excited $^3(\pi,\pi^*)$ triplet states). As a rule, the efficiency of the radiationless depopulation path via the triplet manifold in various D−A systems depends on the energy of the $^3(\pi,\pi^*)$ states with respect to that of the ^{1,3}CT states. The lowest triplet T_1 state in the 9-acridyl and 9-anthryl derivatives of aromatic amines is of the $^3(\pi,\pi^*)$ character, the excitation being localized in the acceptor moiety.[26b,28a] Thus, the quantitative analysis of the radiationless transitions in the studied compounds is hardly possible without the understanding of the mechanism of the radiationless depopulation which needs the study (being in progress) of the solvation and temperature effects on the ISC efficiency.

4. Concluding Remarks

Aryl derivatives of aromatic amines emit a single fluorescence band at room temperature. Solvatochromic effects on their spectral position $\tilde{\nu}_{flu}^{CT}$ indicate a dominant CT character of the emitting singlet states. In low-polarity solvents, however, a deviation from the linear correlation between $\tilde{\nu}_{flu}^{CT}$ and the solvent polarity function neglecting the solute polarizability is observed. This effect is most probably related to the dependence of the electronic structure of the fluorescent ^{1}CT(f) states on solvation.

(73) Efrima, S.; Bixon, M. *Chem. Phys. Lett.* **1974**, *25*, 341.

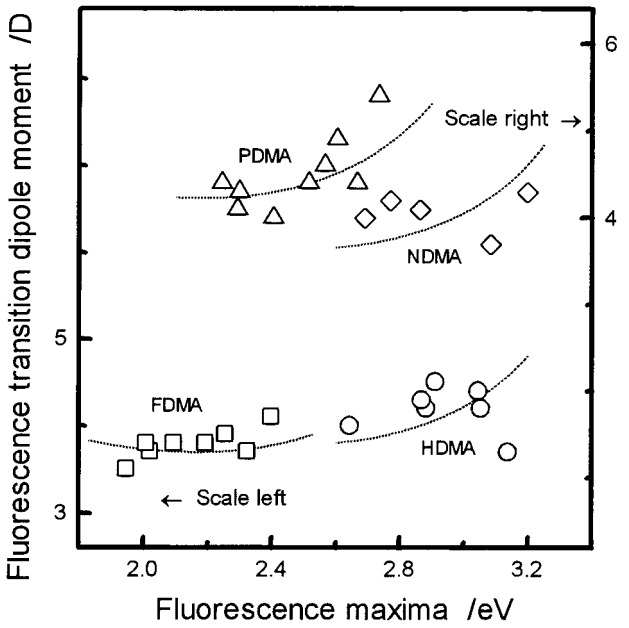

Figure 18. Dependence of the fluorescence transition dipole moments M_{flu} on the energy related to the CT flurescence maxima at room temperature for selected aryl derivatives of *N*,*N*-dimethylaniline: FDMA (squares) and HDMA (circles)—scale left; NDMA (diamonds) and PDMA (triangles)—scale right. The solid lines correspond to the numerical fit according to eq 20 (see text and Table 6).

The analysis of the CT fluorescence profile leads to the quantities relevant for the electron transfer in the Marcus inverted region. Undoubtedly, the important result is related to the dependence of the inner reorganization energy λ_i on solvation. This finding can be explained by the inseparability between the low frequency nuclear motions of the solute (e.g., associated with the torsion around the A−D bond) and the change of the A−D bond order (resulting in the variation of the A−D bond length and the respective angles).

p-Acridyl derivatives of aromatic amines show a low-energy CT absorption band which undergoes a red-shift with increasing solvent polarity. An analysis of the absorption spectra indicates that the appearance of the CT absorption band generates a decrease of the intensity of the $^1L_a \leftarrow S_0$ excitation localized in the acceptor subunit. It points out the importance, in addition to the coupling between charge-transfer and ground states, of the interactions between the ^{1}CT and ^{1}LE state(s). This hypothesis is confirmed by the finding of the dependence of the electronic transition dipole moments M_{flu} corresponding to the CT fluorescence on the solvent polarity. The similar results have been obtained for *p*-anthryl derivatives of aromatic amines.

The comparative determination of M_{abs} (which is related to the $^1CT \leftarrow S_0$ absorption) and M_{flu} made possible to estimate independently the electronic coupling elements between the Franck−Condon ^{1}CT(a) state reached in absorption or the solvent-equilibrated fluorescent ^{1}CT(f) state and the ground state S_0 (V_{0A} and V_{0F}, respectively) or the locally excited ^1L_a state lying most closely in energy (V_{1A} and V_{1F}, correspondingly). In low polarity solvents the significant increase of the interaction elements ($V_{0F} \approx V_{1F}$) related to the fluorescent state with respect to those representing the CT absorption (V_{0A} and V_{1A}) indicates that the molecules are flattened upon excitation. The values of V_{0F} and V_{1F} decrease with the increasing solvent polarity to the values of V_{0A} and V_{1A}. This finding suggests that the compounds in highly polar environment probably do not undergo any significant conformational changes accompanying the excited-state charge separation.

The experimental and computational results led us to propose a simple model which allows one to predict the photophysical behavior of a particular D−A compound from the properties of its donor and acceptor subunits. It has been shown previously[13] that the probabilities of the radiative charge transfer transitions (i.e., the absorption $^1CT \leftarrow S_0$ and fluorescence $^1CT \rightarrow S_0$) for the *N*-carbazoyl derivatives of aromatic nitriles could be correlated with the product of (i) the LCAO coefficients of the acceptor LUMO orbital and the donor HOMO orbital of the carbon atoms forming A−D bond and (ii) $\cos\Theta_{A-D}$, where Θ_{A-D} is the angle between the planes of the acceptor and donor moieties (eq 11a). Moreover, it has been pointed out[13] that such a simple relation was possible to use due to the dominant electronic coupling between the ^{1}CT state and the ground state. The present results indicate that the reasonable prediction of the electronic coupling elements is also possible for the 9-acridyl and 9-anthryl derivatives of aromatic amines, i.e., for the D−A systems for which, in addition to the interaction elements V_0 between the ^{1}CT and S_0 states, the electronic coupling elements V_1^A between the ^{1}CT state and the locally excited ^1L_a state lying most closely in energy have to be taken into account (cf. eqs 11a and 11b). In these particular systems the ^1L_a state is related to the acceptor subunit due to the relatively large energy gap $E_{LE}^D - E_{LE}^A$ (being higher than 5000 cm^{-1} for all the studied compounds except BDMN and ADMN)[51,52,65] between the lowest transitions $^1(\pi,\pi^*) \leftarrow S_0$ in the acceptor and donor (aromatic amine) moieties. In order to test our hypothesis for other D−A systems we have selected some aryl derivatives of *N*,*N*-dimethylaniline which show the CT fluorescence: NDMA,[28,74] PDMA,[28,75] HDMA,[29] and FDMA[28] (Figure 3). The ^1L_a states of FDMA and PDMA associated with the acceptor (aryl) subunit[65,76,77] are lower than those connected with the donor moiety.[65] For NDMA and HDMA the sequence of the ^1L_a states is opposite.[65,78,79] Moreover, the values of $|E_{LE}^D - E_{LE}^A|$ are much smaller for FDMA, HDMA, NDMA, and PDMA than those for the D−A acridine and anthracene derivatives. Due to these facts, the transition dipole moments M_{flu} have to be discussed in terms of the electronic coupling between the ^{1}CT state and the ground state (V_{0F}), or locally excited states ^1L_a for both of those of the acceptor (V_1^A) and of the donor (V_1^D)

$$M_{flu} \approx V_{0F}\Delta\mu/hc\tilde{\nu}_{flu}^{CT} + V_1^A M_{LE}^A/(E_{LE}^A - hc\tilde{\nu}_{flu}^{CT}) + V_1^D M_{LE}^D/(E_{LE}^D - hc\tilde{\nu}_{flu}^{CT}) \quad (20)$$

where M_{LE}^A and M_{LE}^D denote the transition dipole moments corresponding to the radiative transition $^1L_a \leftarrow S_o$ in the acceptor or donor, respectively. The values of M_{LE}^A for phenyl substituted fluoranthene (≈4.4 D), naphthalene (≈3.7 D), pyrene (≈5.0 D),[35] and phenanthrene (≈3.7 D),[29] and that of M_{LE}^D for *N*,*N*-dimethylaniline (≈4.3 D)[35] were obtained from the respective absorption and/or fluorescence data (cf. Table 5 in ref 28b). In order to estimate the electronic coupling elements V_{0F}, V_1^A, and V_1^D from the experimental transition dipole moments M_{flu} in various solvents[28,29,74,75] by the fitting procedure according to eq 20, it has been assumed that all the electronic coupling

(74) Results of the photophysical investigations of the naphthyl derivatives of aromatic amines will be published shortly.

(75) Wiessner, A.; Hüttmann, G.; Kühnle, W.; Staerk, H. *J. Phys. Chem.* **1995**, *99*, 14923.

(76) (a) Kolc, J.; Thulstrup, E.W.; Michl, J. *J. Am. Chem. Soc.* **1974**, *96*, 7188. (b) Dalgaard, G.P.; Michl, J. *J. Am. Chem. Soc.* **1978**, *100*, 6867.

(77) (a) Vasák, M.; Whipple, M. R.; Berg, A.; Michl, J. *J. Am. Chem. Soc.* **1978**, *100*, 6872. (b) Waluk, J. W.; Michl, J. *Anal. Chem.* **1981**, *53*, 236.

elements are similar $V(\text{exp}) \approx V_{0F} \approx V_1^A \approx V_1^D$ (Figure 18). In Table 6 the values of $V(\text{exp})$ corresponding to the best fit of the experimental data are compared with those calculated from the relation

$$V(\text{calc}) = C^A C^D \beta_{CC} \cos(\Theta_{A-D}) \qquad (21)$$

The simplified expression 21 results from eqs 11a, 11b, and 11c since the LCAO coefficients of the $2p_z$ atomic orbitals at the carbon atoms forming A−D bond are similar for a given acceptor ($C^A_{HOMO} \approx C^A_{LUMO}$) as well as the donor ($C^D_{HOMO} \approx C^D_{LUMO}$). The results were obtained assuming the value of the resonance integral and that of the angle between the planes of the acceptor and donor subunits $\Theta^G_{A-D} = 55(\pm 5)°$ (as computed by AM1 and molecular mechanics[59] methods). It may be interesting that X-ray investigations of 4-(1-naphthyl)-*N*,*N*-diethylaniline[80] lead to the value of Θ^G_{A-D} as 58.7°. The agreement between the values of $V(\text{exp})$ and $V(\text{calc})$ may be regarded as satisfactory (Table 6).

Table 6. Experimental $V(\text{exp})$ and Calculated $V(\text{calc})$ Electronic Coupling Elements for Selected Aryl Derivatives of *N*,*N*-Dimethylaniline

compd	$C^A_{HOMO} \approx C^A_{LUMO}$ [a]	$V(\text{calc})$,[b] eV	$V(\text{exp})$,[c] eV
FDMA	0.35	0.20	0.18
PDMA	0.35	0.20	0.18
HDMA	0.39	0.23	0.19
NDMA	0.42	0.24	0.21

[a] Values calculated by AM1 method (that corresponding to *N*,*N*-dimethylaniline is $c^D_{HOMO} \approx c^D_{LUMO} = 0.44$). [b] Calculated from eq 21 with $\beta_{CC} = 2.30$ eV and $\Theta^G_{A-D} = 55(\pm 5)°$. [c] Obtained from the CT fluorescence data and the use of eq 20 assuming $V(\text{exp}) \approx V_{0F} \approx V_1^A \approx V_1^D$.

We are currently investigating D−A aromatic systems which probably allow us to test this simple model both for the fluorescent ^{1}CT states and the lowest ^{3}CT triplet states.

Acknowledgment. This work was sponsored by grant 3 T09A 127 08 from the Committee of Scientific Research. Technical assistance from Mrs. A. Zielińska is deeply appreciated.

JA972474C

(78) (a) Vasák, M.; Whipple, M. R.; Michl, J. *J. Am. Chem. Soc.* **1978**, *100*, 6838. (b) Whipple, M. R.; Vasák, M.; Michl, J. *J. Am. Chem. Soc.* **1978**, *100*, 6844.

(79) Vasák, M.; Whipple, M. R.; Michl, J. *J. Am. Chem. Soc.* **1978**, *100*, 6867.

(80) Tseng, J. C. C.; Huang, S.; Singer, L. A. *Chem. Phys. Lett.* **1988**, *153*, 401.